Applied Physics Reviews

REVIEW ARTICLE | DECEMBER 21 2021

Electrolyte-gated carbon nanotube field-effect transistor-based biosensors: Principles and applications

Bajramshahe Shkodra ; Mattia Petrelli ; Martina Aurora Costa Angeli ; Denis Garoli ; Nako Nakatsuka ; Paolo Lugli ; Luisa Petti

Appl. Phys. Rev. 8, 041325 (2021)
https://doi.org/10.1063/5.0058591

Applied Physics Reviews REVIEW scitation.org/journal/are

Electrolyte-gated carbon nanotube field-effect transistor-based biosensors: Principles and applications

Cite as: Appl. Phys. Rev. 8, 041325 (2021); doi: 10.1063/5.0058591
Submitted: 31 May 2021 · Accepted: 18 October 2021 ·
Published Online: 21 December 2021

Bajramshahe Shkodra,[1] Mattia Petrelli,[1,a)] Martina Aurora Costa Angeli,[1] Denis Garoli,[2] Nako Nakatsuka,[3] Paolo Lugli,[1] and Luisa Petti[1]

AFFILIATIONS

[1]Faculty of Science and Technology, Free University of Bozen-Bolzano, P.zza Università 1, 39100 Bozen, Italy
[2]Istituto Italiano di Tecnologia, Via Morego 30, 16163 Genova, Italy
[3]Laboratory of Biosensors and Bioelectronics, ETH Zurich, Gloriastrasse 35, 8092 Zurich, Switzerland

[a)]Author to whom correspondence should be addressed: mattia.petrelli@unibz.it

ABSTRACT

Nowadays, there is a high demand for sensitive and selective real-time analytical methods suitable for a wide range of applications, from personalized telemedicine, drug discovery, food safety, and quality control, to defense, security, as well as environmental monitoring. Biosensors are analytical devices able to detect bio-chemical analytes (e.g., neurotransmitters, cancer biomarkers, bio-molecules, and ions), through the combination of a bio-recognition element and a bio-transduction device. The use of customized bio-recognition elements such as enzymes, antibodies, aptamers, and ion-selective membranes facilitates achieving high selectivity. Among the different bio-transduction devices currently available, electrolyte-gated field-effect transistors, in which the dielectric is represented by an ionic liquid buffer solution containing the targeted analyte, are gaining increasing attention. Indeed, these bio-transduction devices are characterized by superior electronic properties and intrinsic signal amplification that allow the detection of a wide range of bio-molecules with high sensitivity (down to pM concentration). A promising semiconducting material for bio-transduction devices is represented by carbon nanotubes, due to their unique electrical properties, nanosize, bio-compatibility, and their simple low-cost processability. This work provides a comprehensive and critical review of electrolyte-gated carbon nanotube field-effect transistor-based biosensors. First, an introduction to these bio-sensing devices is given. Next, the device configurations and operating principles are presented, and the most used materials and processes are reviewed with a particular focus on carbon nanotubes as the active material. Subsequently, different functionalization strategies reported in the literature, based on enzymes, antibodies, aptamers, and ion-selective membranes, are analyzed critically. Finally, present issues and challenges faced in the area are investigated, the conclusions are drawn, and a perspective outlook over the field of bio-sensing technologies, in general, is provided.

TABLE OF CONTENTS

I. INTRODUCTION

Biosensors are analytical devices that transduce (i.e., convert) a bio-chemical response caused by a specific analyte or a group of

analytes into a measurable signal proportional to the target analyte(s).[1,2] To realize a functional biosensor, two key elements are necessary: (i) the bio-recognition element (such as enzymes, antibodies, aptamers, and ion selective membranes) and (ii) the bio-transduction device, which converts the interaction(s) between the bio-recognition element and the analyte(s) of interest (input signal) into a measurable (output) signal. Output signals can then be further manipulated, ideally including on a single platform both the sensing element and the readout circuitry.[3] In the last decades, different bio-transduction devices have been used, including optical,[4] piezoelectric,[5] and electrochemical approaches.[6] Among those, electrochemical devices (where the bio-chemical input signal is converted into an electrical output signal) are heavily investigated due to their fast response time (few seconds),[7] easy miniaturization, and no need of sample pretreatment.[8] The resulting label-free detection strategy (i.e., no need to attach fluorescent or radioactive molecules to the targeted analyte(s) to perform the measurements)[9–11] enables integration into low-cost miniaturized portable systems, allowing both laboratory analysis and point-of-care testing.[12] These advantages facilitate the use of biosensors in diverse fields such as biomedicine and health care,[10,13–17] wearable electronics,[18,19] food and beverage quality control,[15,20,21] circuit applications,[22] and precision agriculture.[23,24]

Biosensors using field-effect transistors (FETs) as bio-transduction elements are one of the most promising class of electrochemical devices. Superior electronic properties and intrinsic signal amplification allow FET-based biosensors to detect a wide range of bio-molecules with high sensitivity and selectivity.[12,25–27] In general, in FETs, the flow of electrons (or holes) through the semiconducting channel connecting the two conductive (source and drain) terminals is controlled via the third (gate) electrode, allowing current variations over many orders of magnitude.[8] In addition to the classical gate contact control, the charge carrier flow in FETs can also be perturbed via multiple mechanisms involving surface effects, local electric fields, and chemical reactions in the bulk.[28] FET-based biosensors rely on these latter mechanisms, where changes in the electrostatic surface potential induced by the specific binding of the analyte molecule(s) to the bio-recognition elements (intimately integrated in the FET transduction platform) are used to detect the analyte(s) of interest.[8] Specific examples of electrochemical biosensors using FET transduction can be found in several recent papers.[10,13–17,20,21,23,29–32]

To date, the most widely used FET technology is constituted by the so-called metal-oxide-semiconductor FETs (MOSFETs), where the gate contact is insulated from the silicon (Si) semiconducting channel by a thin silicon dioxide (SiO_2) layer.[33] FET-based biosensors can be realized using different device configurations such as so-called back-gated (BG-FET),[34,35] dual-gated (DG-FET),[36,37] or electrolyte-gated FETs (EG-FETs).[16,38] Among these, EG-FETs, where the typical FET structure is modified by replacing the SiO_2 insulator with an electrolyte such as a solid polymer,[39,40] an ion-gel,[41] or a water-based electrolyte,[42,43] are widely employed bio-sensing FET configurations. Among those, water-based electrolytes are the most used, due to the fact that the majority of the biological analytes can be found in water-based environments.[14] Limitations of MOSFET technology in terms of large-area and low-cost scalability and applicability to low-temperature flexible, stretchable, and bio-compatible substrates have led to the search for alternative semiconductors such as amorphous metal oxides (AMOs),[44] organic materials,[45] and one-dimensional (1D) or two-dimensional (2D) nanomaterials such as carbon nanotubes (CNTs)[46–48] or graphene.[49,50]

Among the possible materials, semiconducting CNTs are particularly interesting due to their potential advantages related to the electrical properties (e.g., relatively large carrier mobility of the individual CNT as high as 2500 $cm^2\ V^{-1}\ s^{-1}$),[51] the nanometric dimension, biocompatibility with the target analytes,[52] and the solution processability that allows CNTs to be unobtrusively integrated into almost any type of substrate (e.g., flexible polymeric foil).[28,53–55] CNTs are characterized by a unique geometry consisting of a 1D nanosize (comparable to the typically targeted bio-molecules) in which the mass is mostly concentrated on the surface. For this reason, CNTs offer not only a large surface area for the immobilization of the bio-recognition elements, but also a surface charge transport that can be highly influenced by small changes of the surrounding environment. Such unique features allow CNT-based biosensors to be sensitive down to pM concentrations.[56] In that perspective, CNTs are especially attractive to realize EG-FET biosensors (so-called EG-CNTFETs).[57] This is why, in the last decade, manifold applications of EG-CNTFETs have been demonstrated, including the detection of neurotransmitters (e.g., dopamine and glutamate),[3,54] cancer biomarkers (e.g., BT474 and MCF7 breast cancer cells),[58] real-time monitoring of bio-molecules (e.g., lactate and glucose),[14] cellular culture monitoring,[38] and the realization of multi-ion sensor arrays (e.g., H^+, Na^+, K^+, Ca^{2+}, Cl^-, and NO_3^-).[59–61] In addition, soft and mechanically bendable EG-CNTFET-based biosensors are now also possible,[59] paving the way toward biomedical diagnostics, wearable sensors, and implantable devices.[14,59]

While there are several valid reviews focused on the specific operation mechanisms of EG-FETs based on solid electrolytes for use in printed electronics,[40] on the detection mechanism of biological species using CNTFETs,[62] or on the electrical properties of the CNTs semiconducting layer in EG-CNTFET,[63] on the different electrolyte used for EG-FET operation,[64] there is currently no comprehensive and critical review on EG-CNTFET-based biosensors, where the operating principles of such devices and their application are thoughtfully analyzed.

Main aim of this work is to critically review the recent advances obtained with EG-CNTFET-based biosensors based on different bio-recognition elements. First, in Sec. II, the possible EG-CNTFET configurations, the most used materials and processes are presented, followed by a description of the operating principle of the biosensor. Then, in Sec. III, a critical discussion on CNTs as active material for EG-CNTFETs is given. Subsequently, in Sec. IV, the different functionalization strategies utilized for EG-CNTFET biosensors are introduced. Section V is focused on the analysis of the reported literature about EG-CNTFET-based biosensors, specifically biosensors based on enzymes (Sec. V A), antibodies (Sec. V B), aptamers (Sec. V C), and ion selective membranes (Sec. V D) are critically analyzed. Finally, in Sec. VI, present issues and challenges faced in the area are investigated, the conclusions are drawn and a perspective outlook over the field of bio-sensing technologies, in general, is provided.

II. BIOSENSOR CONFIGURATION AND OPERATION

Aim of this section is to give the reader an extensive introduction to the EG-CNTFET bio-sensing platform. Sections II A and II B are dedicated to the discussion of the design and material choices used for EG-CNTFET in literature, while Secs. II C and II D are focused on the description of the working principle behind the operation of an

EG-CNTFET, that is, how to characterize such devices and how this translates in the design and fabrication of a EG-CNTFET-based biosensors.

A. EG-FET configurations

The basic architecture of an EG-FET is, in principle, the same as the one of a conventional FET: it consists of three electrodes, namely, the source, the drain, and the gate. The source and drain electrodes are connected through a semiconducting material, while an insulating material is used to separate the gate electrode from the semiconducting material. By applying a voltage between the gate and source electrodes, it is possible to force the inversion of the region of the semiconductor in close proximity to the oxide, thus forming a conductive channel, so that if a voltage is applied between the source and drain electrodes, the charge carriers (either electrons or holes) can flow through this channel and a current can be measured. The mechanism we just briefly described is referred to as field-effect: through precise control of the voltage applied on the gate electrode, it is possible to modulate the current flowing between source and drain.

In an EG-FET, the insulating material is replaced with an electrolyte solution, that is, a liquid medium (mostly de-ionized water) in which the salt of choice is dissolved, releasing ions and thus forming a conductive solution.[66] In the specific case of EG-CNTFETs, the semiconducting layer is made of CNTs. As it will be explained later in Sec. III, both random and aligned networks are employed, and several growth/deposition techniques are used as well. The most used configurations reported in the literature for EG-FETs are depicted in Fig. 1, while in Table I we have summarized the fabrication details reported for the different platforms. The most used configuration is the one where a conventional reference electrode is used as gate electrode, that is, a commercially available Ag/AgCl needle or a Pt wire [see Fig. 1(a)]. Using a conventional reference electrode helps achieving more stable and reliable performance of the EG-CNTFET, as it will be discussed later in Sec. II B. The other configuration used in the literature is the so-called planar gated EG-CNTFET [sometimes referred to as side gated EG-CNTFET, see Fig. 1(b)]. In this case, the gate electrode is fabricated and patterned together with the source and drain electrodes (i.e., during the same fabrication step). The main advantage offered by this architecture lies in more straightforward fabrication process, since no external elements (and no extra costs) are required for the reference electrode. For the same reason, a completely planar architecture allows for the full exploitation of the properties of flexible, free-standing substrates like polyimide (PI). Albeit typically not reported for EG-CNTFETs, another possible configuration is the so-called extended gated EG-FET [see Fig. 1(c)]. We can divide this configuration in two parts: a CNTFET and a separated gate electrode. The CNTFET here acts as an amplifier for the signal produced by the remote gate electrode. The main advantage offered by the extended gated configuration is the fact that the sensing part of the device is the only one exposed to the environment in which the measurement is performed, and this ensures better stability and reproducibility.[67] In spite of the advantages offered by the latter configuration, in our literature survey we have found very few significant examples of extended gated EG-CNTFETs, the only remarkable one being the one reported by Yamamoto *et al.*[57] It is worth mentioning that some authors, for example, Shibani *et al.*, in their work about cortisol detection,[68] use "EG-FET" as an acronym for extended gated FET, as there is no universal agreement in the field on how to refer to the specific configurations.

B. EG-FET materials and fabrication processes

In this subsection, we briefly describe the different substrates and materials used for the conductive electrodes and the electrolyte dielectric, as reported in Table I. A thorough discussion about the techniques used to grow/deposit the CNTs on the substrate, as well as the properties of the CNTs, is the focus of Sec. III.

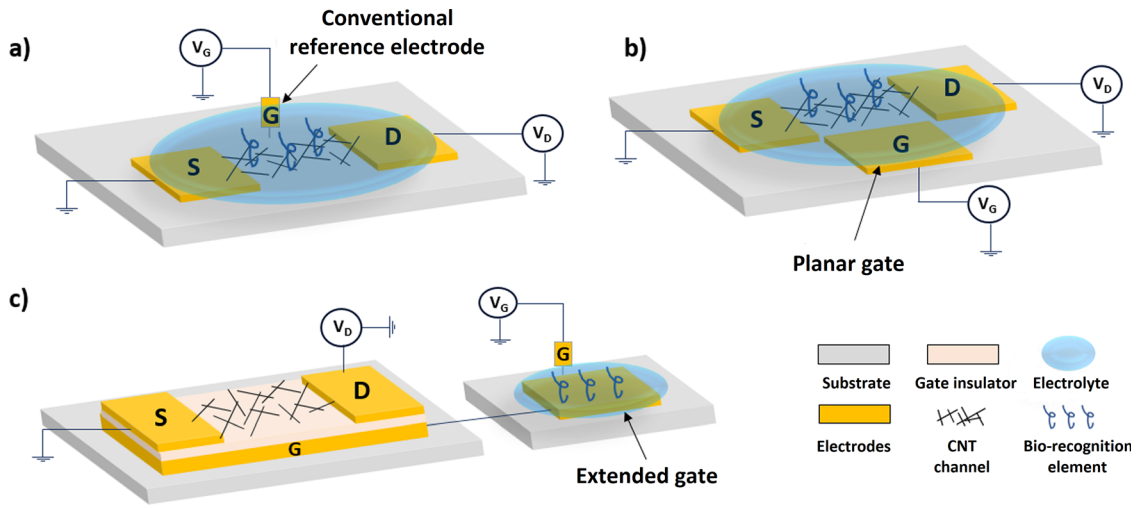

FIG. 1. Schematic representation of biologically sensitive electrolyte-gated carbon nanotube field-effect transistors (EG-CNTFETs): (a) conventional gated (reference electrode) EG-CNTFET, (b) planar gated EG-CNTFET, and (c) extended gate EG-CNTFET. For all the three configurations, the different components are shown: substrate, gate (G), source (S) and drain (D) electrodes, gate insulator, semiconducting CNT channel, electrolyte, and bio-recognition element. V_G and V_D are the gate and the drain voltage, respectively. Reproduced with permission from Joshi *et al.*, "Understanding the influence of in-plane gate electrode design on electrolyte gated transistor," Microelectron. Eng. **199**, 87–91 (2018).[65] Copyright 2018 Elsevier.

TABLE I. Summary of the different fabrication techniques and materials used in the realization of EG-CNTFET-based biosensors. Where clearly stated by the authors, the composition and dilution of the electrolyte used is reported.

CNT process	Substrate	S/D materials	S/D encapsulation	Gate	Electrolyte	Ref.
CVD	Si/SiO_2	Ti/Au	···	$Ag/AgCl$ needle	PBS 1×	56
	Si/SiO_2	$Co/Ti/Au$	···	$Ag/AgCl$ needle	(a) PBS 0.0005× (b) human serum	69
	Si/SiO_2	Au	PMMA	Au planar	PBS 0.05×	70
	Si/SiO_2	Cr/Au	···	Ag wire	$NaCl$	71
	Si/SiO_2	Cr/Au	···	$Ag/AgCl$ needle	PBS 1×	72
	Quartz	Au	···	$Ag/AgCl$ needle	PBS	73
	Quartz	Au	···	$Ag/AgCl$ needle	PBS	74
	Si/SiO_2	Ti/Au	···	$Ag/AgCl$ needle	PBS 1×	75
	Si/SiO_2	Au	PMMA	$Ag/AgCl$ needle	KCl $[10^{-5}:10^{0}]$ M	76
Dielectrophoresis	CMOS chip	Pt	SiO_2/Si_3N_4	$Ag/AgCl$ needle	PBS 1×	3
Dip-coating	SiO_2	Au	Epoxy	$Ag/AgCl$ needle	BRB	77
	PI	Cr/Au	Photoresist AZ 1518	$Ag/AgCl$ needle	tris–HCl [2;20] mM	26
	Si/SiO_2	Cr/Au	···	···	PBS 0.15×	78
	SiO_2	Pd/Au	Photoresist AZ 5214	···	PBS	79
	Glass tube	Ti/Au	···	Pt needle	PBS 1×	80
	SiO_2	Pd/Au	Photoresist DNR-L300	$Ag/AgCl$ needle	NMG	81
	PET	Cr/Au	···	$Ag/AgCl$ needle	PBS 1×	82
Spin-coating	Glass	Cr/Au	···	$Ag/AgCl$ needle	DMEM	38
	PI	Cr/Au	···	Pt wire	$NaCl$, $CaCl_2$, $MgCl_2$, KCl	59
	PI	Cr/Au	···	Pt wire	(a) $NaCl$ 150 mM (b) $NaCl$ 112 mM, $CaCl2$ 0.41 mM, $MgCl_2$ 0.28 mM, (c) $NaCl$ 112 mM, $CaCl_2$ 0.41 mM, $MgCl_2$ 0.28 mM, KCl 3.7 mM	83
Spray-coating	PI	Cr/Au	···	Cr/Au planar	PBS, 0.1×	14
	Si/SiO_2	Cr/Au	···	Ti/Pt planar	PBS, [0.001:10]×	61
	PI	MWCNTs	···	MWCNTs planar	$NaCl$, 0.1 M	84
	PI	Cr/Au	···	Cr/Au planar	PBS, 0.1×	85
	Si/SiO_2	Cr/Au	···	Au planar	KCl, $CaCl_2$, K_2SO_4	86
Vacuum filtration	Si/SiO_2	Pd/Au	···	$Ag/AgCl$ needle	PBS, 1×	87
	Si/SiO_2	Ni/Au	Photoresist SU-8	$Ag/AgCl$ needle	PBS, 1×	88

- **Substrates** The choice of the specific substrate, when the fabrication of a new device needs to be planned, is driven by not only by the application (e.g., the substrate has to be flexible because the device needs to be wrapped around a non-planar surface) but also by the processes that the substrate itself will have to go through along the fabrication (i.e., the maximum temperature that the substrate is able to withstand, the compatibility with the used chemicals).

As shown in Table I, the most used substrate is the well-established Si/SiO_2 wafer,[56,61,69–72,75–79,81,86–88] thanks to its compatibility with both vacuum- and solution-processed deposition techniques for CNTs. Other rigid substrates reported for EG-CNTFETs are quartz,[73,74] and glass.[38] A peculiar application is the one proposed by Lee *et al.*, where the EG-CNTFET is realized directly on a glass tube meant to be used as a probe.[80] Dudina *et al.*, instead, embedded an EG-CNTFET array on a standard CMOS (complementary-MOS) chip, having on the same substrate also the readout circuit.[3]

Several EG-CNTFETs fabricated on flexible substrates are also reported in literature. PI is by far the most used substrate,[14,26,59,83–85] while there is only one reported example of an EG-CNTFET fabricated on polyethylene terephthalate (PET).[82] The main limitation to be faced when using one of these two materials is related to the maximum temperature they can withstand (PI and PET have a glass transition temperature of around

400 and 70 °C, respectively): in fact, there are no reported examples of EG-CNTFETs fabricated on PI or PET when the chemical vapor deposition (CVD) technique is used for the growth of the CNTs on the substrates, since temperatures between 550 and 1000 °C are required (further details about CVD, as well as for the other techniques, are provided in Sec. III).

- **Source and drain electrodes** The choice of the conductive material to be used for the source and drain electrodes is mainly motivated by how well the work function of the material match the one of the semiconducting material, in order to guarantee a low contact resistance. In the specific case of our literature survey, being the semiconducting material CNTs, it is not surprising to notice from Table I that almost all the references report gold (Au) as conductive material for the source and drain pads. Only in the work of Dudina *et al.*, the material of choice is platinum (Pt).[3] Nevertheless, different choices can be made regarding the material for the adhesion layer, usually required because of the poor adhesion of gold on the substrate: the two more used are chromium (Cr)[14,72,78,85] and titanium (Ti).[56,75,80] Palladium (Pd)[79,87] and nickel (Ni)[88] are the two other metals reported. The techniques used for the deposition of the metal pads are electron-beam deposition,[3,69,74,76] thermal evaporation,[14,78,80,85,87] and sputtering,[88] even if it is not uncommon that the details of the fabrication process are omitted. A peculiar approach is the one proposed by Bhatt *et al.*, where the metal pads for source and drain (as well as for the gate, being the EG-CNTFET planar) are substituted with spray-deposited conductive multi-walled CNTs (MWCNTs) pads.[84]
- **Encapsulation of source and drain electrodes** An often overlooked issue is the encapsulation of the metal pads. As it will described later in Sec. II C, the working principle of an EG-CNTFET relies on what happens at the two interfaces between the CNT channel and the electrolyte, and between the gate electrode and the electrolyte. When approaching the fabrication and characterization of an EG-CNTFET, it should be carefully considered also what happens at the interface between the electrolyte and the area of the device where the CNT channel and the metal pads are in contact. As correctly addressed by Yamamoto *et al.*, if the electrical behavior of the interface between CNTs and the metal pads changes consequently to the exposure to the electrolyte, this could become the main phenomenon dictating the performance of the device, instead of the CNT channel itself.[57] This can be also generalized to EG-FETs realized with other semiconducting materials other than CNTs: Sonmetz *et al.*, for example, highlighted that without the encapsulation of the source and drain contacts no EG-FET behavior was possible in their Si-based water-gated transistors.[43] It is hence quite surprising to see in Table I that only very few authors embedded this fabrication step in their workflow. The materials used for the passivation of the pads are mainly photoresists,[26,57,70,76,79,81,88] but we also found an example where an epoxy is used.[77] For their EG-CNTFET array embedded directly in a CMOS chip, Dudina *et al.* used an SiO_2/Si_3N_4 passivation layer to cover the Pt pads. In some cases, like in the work of Lee *et al.*, the encapsulation material is not explicitly mentioned, but it can be seen from the schematic that passivation of the pads was performed as well.[80]
- **Gate electrode** We have already introduced the two main architectures used for the fabrication of EG-CNTFETs: the conventional one, with an external reference electrode, and the planar one. It is quite straightforward to understand how the choice of the architecture directly determines the range of materials that can be used for the gate electrode. For the external gate, the vast majority of the reported literature employs a commercially available Ag/AgCl electrode,[26,38,56,69,72–77,81,82,87,88] that uses a concentrated KCl solution to provide a stable reference potential.[89] The other materials employed for this configuration are Ag, in the form of a wire,[71] and Pt, both in the form of needle[80] and wire.[59,83] When the planar configuration is adopted, the gate electrode is normally realized during the same process step of source and drain, so also the materials used are the same.[14,70,84–86] Nevertheless, there might be cases in which a different material is needed (e.g., to perform the functionalization of the gate electrode) so that a specific step is introduced in the fabrication workflow.[61]
- **Electrolyte** The analytical performance of EG-CNTFETs is mainly demonstrated in phosphate buffer saline (PBS) electrolyte (pH = 7.4), as this is an isotonic solution nontoxic to biomolecules.[3,14,56,57,69,70,72–75,78–80,85,87,88] Commercially available 1× PBS (corresponding to 10 mM phosphate buffer) consists of 137 mM $NaCl$, 2.7 mM KCl, 10 mM Na_2HPO_4, and 1.8 mM KH_2PO_4. Sometimes, instead of PBS, a specific combinations of salts is dissolved in de-ionized water.[59,76,83,84,86] Other mediums (i.e., electrolytes) that are used are tris-hydrochloric acid (Tris-HCl),[26] the Dulbecco's modified Eagle's medium,[38] buffer solutions prepared using the Britton–Robinson methods,[77] and the NMG buffer.[81] Not all the papers state clearly if the medium used is diluted, and in which ratio: as it will be explained in Sec. II C, the choice of the dilution is extremely important during the characterization of the EG-FET as a biosensor. It is also worth highlighting that a control of the dilution of the medium in real-life applications (e.g., real-time monitoring of blood, sweat) is not possible: when the EG-CNTFET biosensor is designed for such applications, the testing of the biosensors should be done in conditions that mimic as much as possible the effective environment in which they will operate. The choice of the specific electrolyte determines also the range of voltages that can be used to operate the EG-CNTFET: in water-based electrolytes, the voltage is in the range of ±1 V as the electrochemical window (i.e., the maximum voltage that can be applied without inducing any oxidation/reduction in the electrolyte) of water is 1.23 V.[90] While such a small range of voltages may constitute a limitation in terms of electrical performance, it becomes an advantage for applications were small voltages are a fundamental requirement (e.g., wearable applications). To ensure that the liquid medium stays only on top of the active area of the device, usually a microchamber is fabricated and placed on top of the EG-CNTFET. The most used material for this is polydimethylsiloxane (PDMS).

C. EG-FET operation

The working principle of EG-FETs relies on the intrinsic properties of the ions contained in the electrolyte to rearrange themselves when an external voltage (i.e., an electric field) is applied, and the consequent formation of two electric double layers (EDLs) at the two interfaces between the gate electrode and the electrolyte and between the CNT channel and the electrolyte: thanks to the formation of the two EDLs, as it will be shortly explained, the bulk of electrolyte

effectively behaves as an insulator, thus enabling a FET-like behavior of the EG-FET.

As depicted in Fig. 2(a), when no bias is applied the cations (positively charged ions) and the anions (negatively charged ions) are randomly dispersed inside the electrolyte. In principle, an EG-FET can be fabricated by using both an n-type semiconducting material (i.e., a semiconductor where the main charge carriers are negatively charged electrons) and a p-type semiconducting material (i.e., a semiconductor where the main charge carriers are positively charged holes). Semiconducting CNTs typically show p-type behavior, since the oxygen present in the air acts as a p-dopant,[91] which means that a negative bias is typically required to turn on the EG-FET, as explained in Sec. II C. Figure 2(b) shows what happens in the electrolyte when a negative bias is applied, that is, a negative voltage is applied between the gate electrode and the source electrode: the cations accumulate at the interface between the gate electrode and the electrolyte, while the anions accumulate at the interface between the CNT channel and the electrolyte. In both cases, a monolayer of ions is formed at the interface between the two materials, immediately followed by a region characterized by an exponential decay of the concentration of ions. This mechanism is known as the Stern-modified Gouy–Chapman double layer model.[92]

Each of the two EDLs behaves, effectively, as a parallel plate capacitor, screening the rest of the ions from the two interfaces. The specific capacitance of an EDL (i.e., the capacitance per unit area, usually reported in $\mu F\,cm^{-2}$) can be then calculated using the Helmholtz equation:[40]

$$c = \frac{k\varepsilon_0}{\lambda_D}, \tag{1}$$

where k is the relative permittivity of the electrolyte, ε_0 is the vacuum permittivity, and λ_D is the width of each of these two EDLs, that is referred to as Debye length. The Debye length can be seen as the distance, considering the solid–electrolyte interface as the starting point, after which the charges are screened by the ions forming the EDL. In an electrolyte solution, the λ_D can be defined using the following formula:[93]

$$\lambda_D = \sqrt{\frac{\varepsilon_0 \varepsilon_r k_B T}{2 N_A q^2 I}}, \tag{2}$$

where ε_0 is the vacuum permittivity, ε_r is the relative permittivity of the medium, k_B is the Boltzmann constant, T is the absolute temperature in kelvin, N_A is the Avogadro number, q is the elementary charge, and I is the ionic strength of the electrolyte expressed in mmol L^{-1}. As all the other parameters are fixed, the ionic strength becomes crucial for the determination of the λ_D: as an example, for 1× PBS the calculated λ_D is 0.7 nm, for 0.1× PBS (i.e., 1 part of 1× PBS plus nine parts of de-ionized water) 2.3 nm, for 0.01× PBS 7.3 nm, while 0.0001× PBS reaches a λ_D of approximately 100 nm.[42]

Two important conclusions can be drawn from the definitions of the specific capacitance and of the Debye length:

- the specific capacitance of an EDL is several orders of magnitude higher than the one of conventional oxides. For example, if we consider a 1× PBS, whose relative permittivity is around 80, we get a specific capacitance of 10 $\mu F\,cm^{-2}$. To have a reference, if we consider a conventional 65-nm-thick SiO_2 oxide[94] (relative permittivity = 3.9), we obtain a specific capacitance of circa 50 $nF\,cm^{-2}$, while for a 50-nm-thick Al_2O_3 oxide[95] (relative permittivity = 9.5) we obtain a specific capacitance of circa 170 $nF\,cm^{-2}$. Having such a bigger capacitance dramatically strengthens the field-effect, that is, the current flowing in the semiconducting channel changes in a measurable way even in response to very small changes of the gate voltage. Moreover, as already mentioned before, having such a big capacitance allows having good electrical behavior even when a very small range of voltages is used for the operation of the EG-FET. The main drawback is represented by the switching speed of the device, which is much slower than conventional MOSFETs, since a bigger capacitance requires more time to be charged/discharged.
- λ_D depends only on the intrinsic properties of the electrolyte, that is, its relative permittivity and the ionic strength. This means that, in first approximation, the electrical properties of the EDLs are determined only by the composition of the electrolyte. This becomes particularly crucial in real-life applications (e.g., sweat for sport-monitoring applications) where there is no direct control over the characteristics of the medium in which the EG-FET will be employed.

Ideally, once the two EDLs are formed at the gate–electrolyte and at the CNT channel–electrolyte interface, there is no voltage drop across the bulk of the electrolyte, so that the ions do not move in response to the applied bias, that is, there is no current flowing between the gate and source electrodes. In other words, thanks to the formation of the two EDLs the bulk of electrolyte effectively behaves as an insulator; hence, an EG-CNTFET can be analytically described using the notation and equations adopted for conventional FETs:

- V_{GS} is the voltage applied between the gate and the source electrodes ($V_{GS} = V_G - V_S$). By controlling the V_{GS}, it is possible to enable the formation of the EDLs, i.e., to turn on the

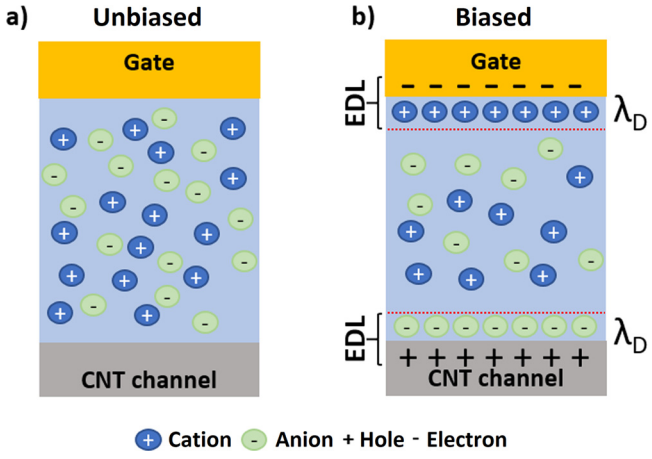

FIG. 2. (a) Unbiased and (b) biased cross section operation of an EG-CNTFET. In particular, with a negative voltage applied between the gate and source electrodes (b), cations accumulate on the gate electrode surface, while anions accumulate at the p-type CNT channel surface. Under these conditions, electric double layers (EDLs) are formed on both the gate electrode surface and the CNT channel establishing the gate dielectric of the FET.

EG-CNTFET. The V_{GS} at which the device turns on is the so-called threshold voltage V_{TH}.

- V_{DS} is the voltage applied between the drain and the source electrodes ($V_{DS} = V_D - V_S$). V_{DS} enables the flow of the charges over time (i.e., of the current) in the CNT channel.
- I_{DS} is the current flowing from the drain to the source electrode.

Being semiconducting CNTs a p-type material, V_{TH} is typically negative, so a more negative V_{GS} is needed to turn on the device, and the I_{DS} is negative as well. While a possible choice would be to use the symbols V_{SG}, V_{SD}, and I_{SD}, here we prefer to stick to the former nomenclature, since it is the one adopted in the vast majority of the papers we report. Nevertheless, to avoid ambiguity we will explicitly refer to the absolute value of the voltages and of the current when needed.

Depending on the V_{GS} and V_{DS} values applied, we can distinguish between two operating regimes for the EG-FET (granted that $|V_{GS}| > |V_{TH}|$):

- for $|V_{DS}| < |V_{GS}| - |V_{TH}|$, we say that the EG-FET is operating in linear regime. The current flowing from drain to source is described by the following equation:

$$I_{DS,lin} = \mu C_{EDL} \frac{W}{L} (V_{GS} - V_{TH}) V_{DS}, \tag{3}$$

where μ is the channel mobility, W and L are the channel width and length, respectively, and the capacitance C_{EDL} is the series of the capacitance C_{GE} of the EDL at the gate–electrolyte interface and the capacitance C_{SE} of the EDL at the CNT channel–electrolyte interface

$$C_{EDL}{}^{-1} = C_{GE}{}^{-1} + C_{SE}{}^{-1}. \tag{4}$$

- for $|V_{DS}| > |V_{GS}| - |V_{TH}|$, we say that the EG-FET is operating in saturation regime. Here, the I_{DS} described as

$$I_{DS,sat} = \mu C_{EDL} \frac{W}{2L} (V_{GS} - V_{TH})^2. \tag{5}$$

The characterization of the EG-FET is then carried out measuring the change in the I_{DS} for several combinations of V_{GS} and V_{DS} applied. We call transfer characteristics the I_{DS}-V_{GS} curves, taken for one or more different values of V_{DS}. We call instead output characteristics the I_{DS}-V_{DS} curves, taken for different values of V_{GS}. Typical transfer and output curves obtained from an EG-CNTFET are depicted in Fig. 3.

From the analysis of the transfer curves it is possible, in principle, to extract several electrical parameters of interest: the carrier mobility μ, the I_{ON}/I_{OFF} ratio, the threshold voltage V_{TH}, the transconductance g_m, the subthreshold swing SS, and the off current I_{OFF}. A thorough description of each of these parameters and how to extract them can be found in the work from Petti *et al.*[44] In the specific case of the EG-CNTFETs, very rarely these parameters are reported by the authors. One exception is the I_{ON}/I_{OFF} ratio, thanks probably to the fact that it is, as highlighted in Fig. 3(a), the most straightforward to extrapolate from the curve: in fact, it is the ratio between the maximum I_{DS} and the minimum I_{DS}. While for conventional FETs typical values are $>10^6 A/A$,[96] for EG-CNTFET the I_{ON}/I_{OFF} ratio is typically between $10^2 A/A$ and $10^3 A/A$, where the limitation comes from the trade-off between the maximum I_{ON} that can be achieved without having an equal increase in the I_{OFF}, due to the conduction mechanism of the CNTs.[94] The other parameter is the V_{TH}, usually obtained from the linear extrapolation of the transfer curve (when the device is operated in linear region) or the linear extrapolation of the $\sqrt{I_{DS}}$-V_{GS} curve (when in saturation regime).

In Sec. II D, we will explain how the electrical characteristics (in particular, the I_{DS}-V_{GS}) can be used to understand the behavior of an EG-CNTFET used as a biosensor.

D. EG-FET as a biosensor

In Sec. II C, the working principle behind the operation of an EG-FET has been described. By using a bio-recognition element, that is, an element able to react only upon exposure to the target of interest,

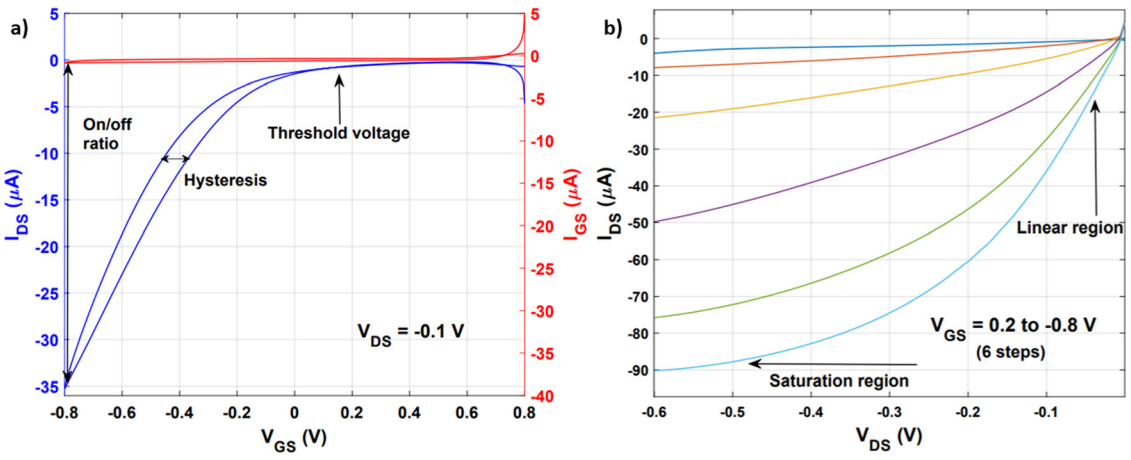

FIG. 3. Typical current–voltage (I–V) characteristics of a p-type EG-CNTFET (L = 50 μm, W = 57 mm): (a) transfer (I_{DS}-V_{GS}), and (b) output (I_{DS}-V_{DS}) curves. The transfer characteristics were recorded by sweeping the V_{GS} from +0.8 to −0.8 V, while keeping the V_{DS} constant at −0.1 V. The I_{ON}/I_{OFF} ratio, hysteresis, and threshold voltage are highlighted. The output characteristics were recorded by sweeping the V_{DS} from 0 to −0.6 V for different values of V_{GS} (from +0.2 to −0.8 V, with −0.2 V steps). The linear and saturation regions are highlighted.

it is possible to use an EG-FET as a biosensor, achieving a selective response to bio-molecules. From the explanation of the working principle of the EDLs, it is straightforward to conclude that for high sensitivity the binding of the analyte to its bio-recognition element should occur within the Debye length, so that the presence of the analyte can actually lead to a change in the behavior of the CNT channel, ultimately leading to a change in the I_{DS}. On the contrary, if the binding occurs at distances bigger than λ_D, the charges will be screened by the EDL, and no actual effect will be observed in the I_{DS}. As we already discussed before, it is possible to increase the λ_D by diluting the electrolyte, but the ratio of the dilution should be carefully chosen. First, in real-life settings normally it is not possible to perform a dilution of the medium in which the EG-FET has to work (e.g., blood, sweat), so having a biosensor that works in a diluted medium is not a guarantee of success when moving to the real environment. Second, reducing the ionic strength of the electrolyte can lead to poor efficiency of the detection process.[70] Assuming that the detection happens within the Debye length, the effect of the presence of the analyte of interest in proximity of the CNT channel can be noticed from the analysis of the transfer characteristics of the EG-CNTFET.

If a shift in the threshold voltage V_{TH} happens (i.e., the transfer curve shifts horizontally), this can be either due to charge transfer between the analyte and the CNT channel (as proposed by Allen *et al.*)[62] or due to electrostatic gating (as proposed by Heller *et al.*).[72] In the former case, the addition of positive charge carriers to the p-type CNT channel shifts the threshold voltage toward more positive values, the opposite for the addition of negatively charge carriers. In the latter case, instead, the adsorption of positively charged species causes electrostatic repulsion of the carriers in the CNT channel (i.e., a de-doping of the CNTs), thus a shift of the threshold voltage toward more negative values, the opposite for the adsorption of negatively charged species. During our literature survey, we have found very few examples of EG-CNTFET-based biosensors where the shift in the threshold voltage is used as parameter,[59,77,83] and in those cases, the authors always propose the electrostatic gating effect as an explanation of the observed shift in the curve.

Most of the works in our analysis report a change in the I_{DS} in response to different concentrations of the analyte of interest. If the absolute value of the I_{DS} decreases, this can be related to a drop of the mobility μ of the carriers because of the surface scattering induced by the presence of the charged analyte in proximity of the CNT channel.[62]

In Sec. II B, we have introduced the problem of the encapsulation of the area where the CNT channel and the metal pads overlap. As discussed by Schroeder *et al.*, the effect of the exposure of this area to the electrolyte is still not fully understood and depends on a variety of factors, such as the metal used, the analyte, and the conductivity of the CNTs.[97] Most importantly, this effect can easily become the predominant mechanism behind the change in the I_{DS}: encapsulation of the interface between the CNT channel and the metal should always be performed to have a reliable bio-sensing platform.

From a practical point of view, the characterization of the EG-CNTFET biosensor is carried out exposing the device to different concentrations of the analyte of interest, while measuring the real-time response of the device (i.e., measuring continuously the I_{DS} at a fixed bias) or taking the transfer curve for each concentration. By extracting the electrical parameter of choice from these curves (I_{DS} or V_{TH}, depending on the specific phenomenon observed) and correlating the values to the concentration of the analyte, the so-called calibration curve can be derived. The slope of the calibration curve is defined as the sensitivity S of the biosensor.

Directly related to the slope of the calibration curve is the limit of detection (LOD), defined as the lowest concentration of the analyte that can be detected with reasonable certainty.[97] It can be formally calculated using the following equation:[98]

$$LOD = 3.3x\frac{SD}{slope}, \tag{6}$$

where SD is the standard deviation of the blank, that is, the standard deviation of the measurements carried out without having the analyte in the electrolyte.

III. BIOSENSOR CHANNEL

In this section, we will briefly describe the main physical and electrical properties of semiconducting CNTs, critically analyzing the different methods used to integrate semiconducting CNTs into EG-FETs, as reported in Table I.

CNTs are allotropes of carbon that can be visualized as hollow cylinders made of either one (single-walled carbon nanotubes, SWCNTs) or multiple (multi-walled carbon nanotubes, MWCNTs) hexagonal graphite planes rolled up around the same axis. Due to their high aspect ratio (length to diameter ratio), which ranges between 10^3 and 10^5, CNTs are classified as 1D nano-materials.[99] Indeed, they have a diameter that varies from 0.4 to 100 nm and a length up to tens of μm.[100] The nanometric dimension (comparable in size to most of the relevant analytes) and the high aspect ratio make CNTs an interesting material for bio-sensing, because of the large surface area offered for the immobilization of the bio-recognition elements, consequently leading to an enhancement of the overall biosensor sensitivity. The whole weight of the nanotubes is concentrated on the surface layers, giving them unique electrochemical and adsorption properties.[101] For example, in SWCNTs, every atom of carbon is exposed to the surrounding environment, leading to a better sensitivity toward any interaction that takes place on the surface.[57,101] Depending on the chirality of the graphite planes, CNTs can exhibit either conductive or semiconducting properties. The electronic properties of CNTs are specified not only by the chirality of the nanotubes but also by the diameter (the bandgap scales inversely with the diameter between 1 and 0.3 eV), by the gas exposure history (e.g., oxygen is a p-type dopant), as well as by the presence of defects and contaminants (e.g., residual catalysts from the deposition process).[102,103] The combination of these electronic and electrochemical features makes semiconducting CNTs promising candidates to realize EG-FET-based biosensors.

The selective synthetics/growth of either metallic or semiconducting CNTs is a great challenge, because of their structural similarities.[104] Up to now, chemical vapor deposition (CVD) is the most established and used technique for semiconductor synthesis, in general,[105] and due to the employment of specific catalysts, CVD is also adopted for the growth of CNTs as well (details on the technique in Sec. III B). For example, Zhang *et al.* presented a CVD technique using tungsten carbide as a catalyst to enrich 80% selectivity for the semiconducting CNTs.[106] Similarly, Zhao *et al.* employed cobalt tungstate as a catalyst and graphene oxide as a supporter for the synthesis of 90% semiconducting CNTs.[107] More details on the different methods for

the selective synthesis of semiconducting CNTs can be found in more specific reviews.[108,109]

In addition to the selective growth, to reach high purity of CNTs (e.g., >99%), sorting strategies and post-processing methods are employed, such as interactions via surface functional groups,[110] conjugated polymer wrapping,[111–113] electrophoresis,[114] and density gradient centrifugation.[115] For example, Liu *et al.* presented an alternative technique based on a multiple-dispersion sorting process to achieve a solution containing semiconducting CNTs with a purity as high as >99.9999%.[112] The authors used a multiple-dispersion sorting process for preparing CNTs of ultrahigh semiconducting purity. First, raw CNTs were dispersed and sorted in toluene solvent by using conjugated PCz (poly[9-(1-octylonoyl)-9H-carbazole2,7-diyl]) molecules. The PCz-wrapped semiconducting CNTs were then redispersed in 1,1,2-trichloroethane, and to achieve the desired purity, these processes were repeated twice.

Nevertheless, increased effort is needed for the synthesis of pure semiconducting CNTs, since the ideal performance (i.e., on–off ratio, hysteresis, gate leakage) of FET devices can be achieved only by using high-quality semiconducting nanotubes.[26]

EG-CNTFETs can be realized using a single semiconducting CNT as an electron channel between the source and the drain electrodes or a network of CNTs.[62] The latter is the most used configuration in EG-CNTFET-based biosensors, and it is made of a large number of CNTs in the form of random and aligned matrix. In Secs. III A and III B, we will explain how to realize these types of networks into devices, critically comparing the overall performances.

When CNTs are employed as a random network, an essential aspect is the conduction mechanism, that is, ruled by the percolative theory, in which the charge carriers flow through the matrix following pathways that are created by the contact between different CNTs. Increasing the quantity of CNTs, the numbers of possible current pathways increase with a consequent increase in the network conductance that follows a percolation power law. Thus, the macroscopic transport mechanism of a random CNT network is related to the number and distribution of the preferential current pathways that depends on the CNT composition (the semiconducting to metallic ratio, i.e., the percentage of semiconducting CNTs that typically ranges between 95 and 99%wt), density, alignment, and film thickness.[117,118] For instance, Jang *et al.* showed that the on/off ratio of a pure semiconducting CNT network decreases with the increase in the network density corresponding to the percolation threshold, due to the enhancement of the junction resistance by increasing the CNT-CNT contacts.[117] This limitation can be solved by employing aligned CNTs, thus preventing the formation of the tube-to-tube contact and leading to higher current flow, ultimately to a higher on/off ratio.[119] Indeed, in aligned networks the current flows through multiple tubes that act as parallel and independent channels.

There are several methods available to deposit the CNT channels of EG-CNTFETs, either using vacuum- or solution-based techniques. While vacuum-based methods rely mainly on chemical vapor deposition (CVD),[70,71,99] solution-based techniques include various processes such as drop-casting,[120] dip-coating,[26,78,81] spray-coating,[14,54,84] vacuum filtration,[87,88] spin-coating,[38,59] and dielectrophoresis.[35,77,121] In any case, solution-based techniques also rely on vacuum-based processes, as the methods employed to synthesize CNTs are arc-discharge, laser ablation technique, or CVD. However, nowadays it is easy to find on the market CNT powders with different characteristics, overcoming the need for expensive machines for the synthesis. The so-formed CNTs are then dispersed in an medium such as a water-surfactant-based solution (e.g., sodium dodecyl sulfate or sodium carboxymethyl cellulose) or in an organic solvent (e.g., isopropanol or ethanol) and subsequently solution-deposited on the devices. Compared to vacuum-deposition methods, solution-based techniques offer cost-effectiveness, scalability to large areas, and compatibility with a wide variety of substrates including flexible substrates such as PI and PET.[59,85]

Depending on the deposition method used, either random[84] [see Fig. 4(a)] or aligned[74,104,122] [see Fig. 4(b)] networks of CNTs can be realized. Controlling the alignment and density of the CNTs is an important aspect because it has been proven that the electrical properties of the CNT films are generally dominated by the possible presence of metallic CNTs in the network and by the contact resistance between the tubes. As a matter of fact, a monolayer of aligned CNTs minimizes the tube-to-tube contact resistance and thereby improves the transconductance,[51] leading to an effective mobility up to ten times higher.[76,123]

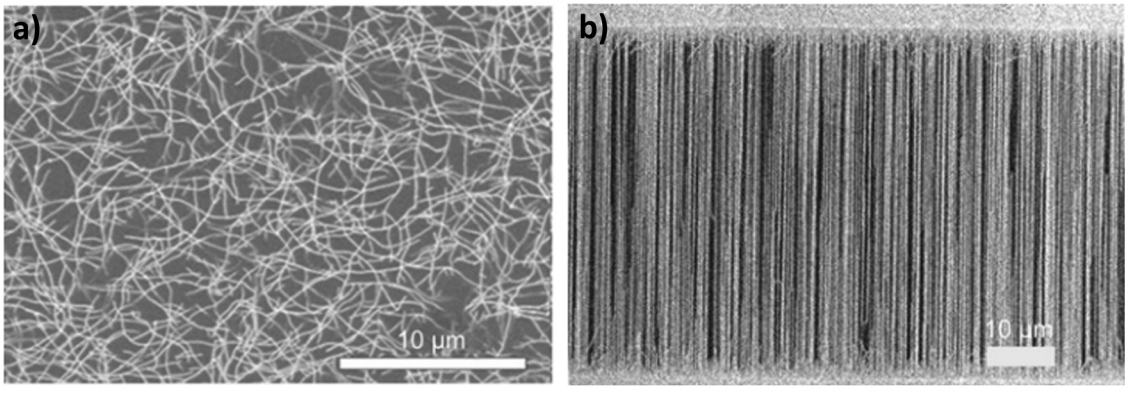

FIG. 4. Scanning electron microscopy (SEM) images of SWCNT thin films grown by chemical vapor deposition (CVD) technique, using Fe as a catalyst, patterned on a quartz substrate: (a) random SWCNT network; (b) perfectly aligned SWCNT network. Reproduced with permission from Cao and Rogers, "Random networks and aligned arrays of single-walled carbon nanotubes for electronic device applications," Nano Res. **1**, 259–272 (2008).[116] Copyright 2008 Authors, licensed under a Creative Commons Attribution (CC BY-NC 2.0) license.

The improvement of the overall electrical performance of the FET results in enhanced sensing properties, leading thus to more efficient biosensors. Although the outstanding properties aligned networks can achieve, EG-FET-based biosensors (and, in general, devices) based on random CNTs are more popular because of their easier manufacturability using cost-effective solution-based techniques, and because of the resulting higher device-to-device reproducibility. In fact, nowadays it is still a challenge achieving a good control of the CNT alignment.

In Secs. III A and III B, we will shortly review the different methods that allow achieving random and aligned networks of CNTs for EG-FETs.

A. Random carbon nanotube networks

Random networks of CNTs are typically achieved using solution-based methods such as drop-casting, dip-coating, vacuum filtration, spin-coating, and spray coating.

Drop-casting represents the cheapest and easiest method to realize random networks of CNTs: the prepared CNT solution is simply drop-cast between the source and drain electrodes using a micropipette. Another simple approach to realize a random network of CNTs is dip-coating. In this case, a patterning of the CNTs is possible through the use of a self-assembled monolayer (SAM) of non-polar organic compounds (e.g., octadecyltrichlorosilane) that blocks the nonspecific adsorption of CNTs. First, the SAM is patterned via photolithography, leaving the space between the source and drain uncovered; then, the device is dipped in the CNT dispersion, and finally, the CNTs are adsorbed onto the uncovered region of the substrate between the source and drain to form the semiconducting channel, while the SAM-coated region remains free of CNTs.[78,79]

Other easy routes for fabricating random networks of CNTs from the dispersion are vacuum filtration and spin-coating. In the case of vacuum filtration, a diluted CNT dispersion is filtered through a membrane filter using a vacuum filtration apparatus forming a continuous thin film of random CNT network.[87,88] Alternatively, spin-coating employs the centripetal force to distribute the CNT dispersion over the substrate surface. The CNTs adhere to the surface via physisorption. However, it may be essential to first coat the substrate with a silane-based SAM or to perform oxygen plasma, to promote adhesion between the CNTs and the substrate.[59] The spinning process can be repeated several times to reach the desired homogeneity and thickness.[38] Interesting is also the possibility to use this technique to realize spin-aligned CNT networks by simply tuning the spin speed.[119] The main drawbacks of these techniques are the low reproducibility, high inter-sample variability, and the formation of non-homogeneous CNT films.

For optimal EG-CNTFET operation, the semiconducting random network should be de-bundled and have a homogeneous tube density. Those optimum conditions can be achieved by using the spray-coating technique. This technique consists of the homogeneous deposition of liquid droplets onto the target substrate starting from a bulk dispersion. The CNT dispersion is decomposed into small droplets (atomization) at the nozzle of the spray head with the aid of a compressed air stream (air-assisted atomization) or kinetic energy (ultrasonic atomization), and deposited onto the substrate. Then, the dispersing fluid is evaporated by heating (the temperature is regulated depending on the boiling point of the solvent), thus leaving the colloidal deposit to form a thin coating.[124,125] In this case, CNT patterning can be realized using a shadow mask that leaves the desired pattern to be sprayed uncovered. Major spray parameters such as material flow rate, nozzle-to-sample distance, motion speed, atomizing gas pressure, and substrate temperature can be adjusted to obtain the desired spray characteristics.[126] This technique is attracting increasing interest in this area, because of its advantages such as easy scalability and fine control of the layer thickness down to tens of nanometers.[94] Indeed, the possibility to obtain thin layers of random network of CNTs allows to effectively reduce metallic pathways of the semiconducting channel, leading thereby to better on/off ratios.[51]

B. Aligned carbon nanotube networks

Although all of the aforementioned deposition methods are widely used, for better EG-CNTFET performance, a semiconducting channel made of highly aligned CNTs is preferred. Indeed, such a structure avoids the tube-to-tube contacts, allowing FETs made of CNT network to approach the intrinsic electrical properties of FETs made by individual CNT (e.g., intrinsic mobility close to the value of a single CNT, around 2500 $cm^2\,V^{-1}\,s^{-1}$).[127] Aligned CNT semiconducting channels can be realized by using both CVD and dielectrophoresis techniques.

As mentioned CVD is the most widely used technique to grow nanomaterials, including CNTs, on rigid substrates. The nanomaterial precursors react on the substrate in a vacuum chamber at high temperatures (550–1000 °C), leading to the formation of a solid film on the substrate.[128,129] This process usually employs a catalyst, typically based on metallic particles (e.g., Ni, Fe, or Co).[129] In the case of CNTs, the carbon source is a hydrocarbon material, its decomposition is catalyzed by a metal atom in a temperature- and pressure-controlled chamber enabling the *in situ* formation of CNTs onto selected substrates such as Si/SiO_2 and quartz.[128–131] Using CVD techniques, it is possible to produce large quantities of CNTs with high purity, and restricted defects, as well as with vertical alignment.[74,128,130] Moreover, the average length of the CNTs and density of the produced films can be controlled by varying different parameters, such as the hydrocarbon materials, the temperature of the reaction, the growth time, and the size of the catalytic particles. The drawbacks of this technique are the high thermal budget, which limits the types of substrates that can be used, and the high fabrication costs (mainly related to the maintenance cost of the machine).[128] Indeed, nowadays it is possible to buy CNT powders with different characteristics (e.g., different lengths, purity, functionalized with the carboxyl groups) that remove the need to synthesize and post-process (e.g., purification, sorting) the CNTs in the laboratory lowering the overall production costs of the devices.

Alternatively, a versatile low-cost technique able to manipulate CNTs into an aligned network is dielectrophoresis. Dielectrophoresis refers to the movement of polarizable particles suspended in a dielectric medium by using a non-uniform electric field.[131] The dielectrophoresis is ruled by the difference of dielectric properties of the CNTs and the surrounding medium (solvent), and it can be tuned and optimized by adjusting several parameters such as deposition time, amplitude, frequency of the alternating current, and solution concentration.[132,133] As a simple low-cost, low-temperature, and scalable method, dielectrophoresis has been widely used for the fabrication of several of EG-CNTFETs.[3,35,77,132]

IV. BIOSENSOR FUNCTIONALIZATION

Prior to any functionalization of the EG-CNTFET structure with the immobilization of a specific bio-recognition element, the device is, in general, characterized by a low selectivity toward any specific analyte. The key component for sensitive and selective EG-CNTFET-based biosensors is the bio-recognition element. The specific operating principles of typical bio-recognition elements (namely, enzymes, antibodies, aptamers, and synthetic ion-selective membranes) together with specific biosensor examples using each of these elements will be reviewed in Secs. V A–V D. Here, we will discuss the functionalization strategies that can be employed to immobilize these bio-receptors onto EG-CNTFET bio-sensing platforms, while also critically comparing the different bio-recognition elements.

A. Functionalization methods

The functionalization step is critical to achieve a specifically readable biosensor (output) signal that correlates directly to the target molecule(s) of interest. As already anticipated in Sec. II, the main strategies used to functionalize an EG-CNTFET-based biosensor include the functionalization of the semiconducting CNT channel, the gate electrode, or the substrate surface.

- **Functionalization of the semiconducting CNT channel** The functionalization of the semiconducting layer is the most employed approach. It can be performed through either non-covalent or covalent surface modifications of the CNTs, leading to either direct immobilization of the analyte or indirect immobilization (i.e., through the use of an additional binding molecule). The non-covalent functionalization consists in the nonspecific physical adsorption of bio-recognition elements onto the CNTs that can involve $\pi - \pi$ interactions, hydrophobic, or electrostatic interactions.[134,135] The covalent functionalization of the CNTs, instead, involves a chemical attachment of functional groups such as carboxyl, amine, and thiol that react with the complementary group present on the bio-molecules, thus forming covalent bonds. In most cases, oxygen-containing groups (e.g., -COOH) are introduced using a strong oxidizing agent (e.g., mixture of sulfuric acid and hydrogen peroxide) on the CNT surfaces, and subsequently activated via 1-Ethyl-3-(3-dimethylaminopropyl)carbodiimide/N-Hydroxysuccinimide (EDC/NHS) or sulfo-NHS yielding a semistable amine-reactive NHS-ester group.[3] Once exposed to the bio-recognition element, the NHS-ester reacts with primary amines (groups that can be found in most of the bio-recognition elements) to form a strong and stable amide bond [see Fig. 5(a)].[78,136] Covalent conjugation provides a stronger and more durable bond, which can interfere with the CNT electronic structure. Indeed, the procedure of generating covalent bonds on the CNT surfaces (e.g., the employment of a strong acid) can generate defects in the nanotube backbone. In fact, the main advantage of the non-covalent functionalization is that the carbon atoms in the nanotubes keep their sp^2 hybridization and the electrical properties of CNTs remain undamaged.[26,97,137] In addition to the direct immobilization described above, indirect immobilization through the use of binding bio-molecules attached to the CNTs (with both covalent and non-covalent bonds) facilitates the subsequent immobilization of the bio-recognition elements. Using binding molecules [such as

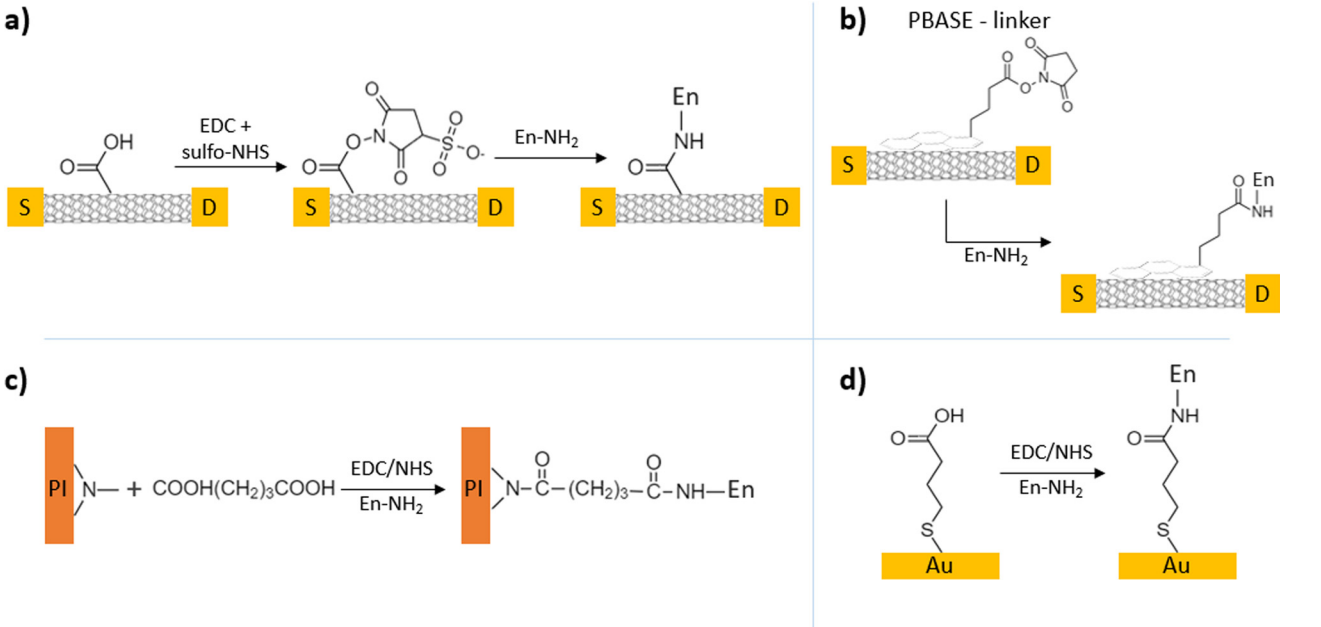

FIG. 5. Different bio-functionalization mechanisms for EG-CNTFETs: (a) direct covalent immobilization of the bio-recognition element (En = enzyme) onto a carboxylated SWCNT—activated via 1-ethyl-3-(3-dimethylaminopropyl)carbodiimide/sulfo-N-hydroxysuccinimide (EDC/sulfo-NHS),[3] (b) indirect covalent immobilization of the bio-recognition element onto the surface of a SWCNT via PBASE (1-pyrenebutyric acid N-hydroxysuccinimide ester) linker molecule,[69] (c) polyimide (PI) substrate functionalization with the bio-recognition element using glutaric acid as a linker molecule,[14] (d) gold gate functionalization with the bio-recognition element using 3-mercaptopropionic acid (3-MPA) as a linker molecule.[85]

1-Pyrenebutyric acid N-hydroxysuccinimide ester (PBASE), and diazonium salts][52,79] with two different functional groups at the two ends enables a non-covalent attaching of the molecule to the CNTs, while the other end is used for covalent coupling to the bio-recognition element [see Fig. 5(b)].[26,73,80]

- **Functionalization of the substrate** Recently, Joshi *et al.* proposed an innovative functionalization approach based on the modification of the PI substrate surface below the semiconducting CNTs channel.[14] In this case, glutaric acid was used as a binding molecule, where one carboxylic end was used to bond to the nitrogen end of the PI substrate, while the other carboxylic end remained free to bond to the amine group of the bio-recognition element [see Fig. 5(c)]. A major advantage of such an approach is the preservation of the structural and electrical properties of the semiconducting CNTs.
- **Functionalization of the gate electrode** The attachment of the bio-recognition element on the gate electrode allows achieving the preservation of the structural and electrical properties of the semiconducting CNTs. In case of gold gate electrodes, thiol chemistry is used for direct immobilization of bio-recognition elements. Indeed, alkanethiols are able to introduce a self-assembled monolayer into the gold surface, due to the high affinity of thiol groups to conjugate with gold. Bhatt *et al.* demonstrated the functionalization of the planar gold gate electrode of an EG-CNTFET using 3-mercaptopropionic acid (MPA) as a linker molecule. The thiol group of MPA was covalently bound to the gold surface, while the carboxylic groups remained free to bind to the amine group of the bio-recognition element [see Fig. 5(d)].[85]

Several strategies for the immobilization of the bio-recognition elements onto the EG-CNTFETs are presented above. What is lacking in the literature is the confirmation of these functionalization strategies. In most cases, the assessment of successful immobilization comes from the electrical measurements (e.g., I–V characteristics). However, while such measurements indicate changes of surface properties, a precise technique should be employed to validate the chemistry used and subsequently quantify the surface coverage and the density of the bio-recognition element. To determine robust functionalization (e.g., surface coverage) by the bio-recognition elements, one can rely on several techniques such as optical waveguide lightmode spectroscopy (OWLS),[138] quartz crystal microbalance (QCM),[139] x-ray photoelectron spectroscopy (XPS),[140] and fluorescence microscopy.[141]

OWLS is an optical *in situ* technique capable of monitoring changes in the polarizability density, that is, in the refractive index, in the proximity of the waveguide surface when exposed to different solutions (e.g., bio-recognition elements).[138,142] Optical waveguides consist of a highly transparent material such as silicon oxide (SiO_2), titanium oxide (TiO_2), and tantalum oxide (Ta_2O_5). The waveguiding layer is further modified by a nanometer-thin layer, allowing the study of biomolecular interaction with specific substrate chemistries. The changes in the refractive index can be used to calculate the surface adsorbed mass density using the de Feijter's formula:[138]

$$m_{adsorbent} = d_{film}\frac{n_{film} - n_{solvent}}{dn/dc}, \tag{7}$$

where d_{film} and n_{film} are the thickness and the refractive index of the added thin film, respectively, $n_{solvent}$ is the refractive index of the medium, and dn/dc the refractive index increment.

Similarly, QCM is a mass-sensitive technique based on an oscillatory quartz crystal capable of detecting nanogram changes in mass. The QCM method employs the piezoelectric property of quartz crystals to measure enormously low mass changes per unit area. By applying an alternating electric current to the quartz crystal, an acoustic oscillation is produced. The frequency of this oscillation is dependent on the thickness of the crystal. When the bio-recognition elements adsorb on the crystal and thus increase the crystal thickness, the instrument will detect the frequency change, and subsequently, the mass of adsorption can be calculated. A detailed description of the technique and its application for monitoring in real-time bio-molecule immobilization can be found in the review by Cheng *et al.*[139]

XPS analysis is a powerful measurement technique widely used to analyze surface chemistries, thus employed also for the monitoring of the bio-molecules immobilization. For example, Tsang *et al.* have confirmed the presence of the PBASE molecule on the graphene channel by analyzing the intensity of N1s peak: since the only source of nitrogen atoms in functionalized graphene is the PBASE molecule, the increase in intensity of the nitrogen peak validated the PBASE immobilization.[140] Further increase in N1s peak was observed after antibodies were immobilized (anti-CD63 antibodies), due to the presence of the amine groups, hence confirming the successful immobilization of the antibodies.

Another technique that could be used to confirm the functionalization and the coverage by the bio-recognition element is fluorescence microscopy. For example, Haddad *et al.* have visualized the biotin attachment to the CNTs via fluorescence microscopy, where the fluorescence intensity is related to the amount of biotin immobilized into the nanotubes.[141] A useful approach consists in labeling the already immobilized bio-recognition element with a fluorophore (which binds specifically to the bio-recognition element) and, afterward, measuring the fluorescence intensity. Using this approach, it is possible to confirm the successful immobilization and, at the same time, gain information about surface coverage, uniformity, and density of the immobilized bio-recognition element.

B. Bio-recognition elements

The aforementioned different functionalization strategies are used to realize EG-CNTFET-based biosensors through the immobilization of the different bio-recognition elements (enzymes, antibodies, aptamers, or synthetic elements like ion-selective membranes), which we will review one by one here. Table II gives details and examples of the most used bio-recognition elements for various applications of EG-CNTFET-based biosensors. Furthermore, the pros and cons of each specific bio-recognition element are listed as well.

Enzymes and antibodies are protein-based bio-recognition elements, often used thanks to their high sensitivity (detection down to nM range) and commercial availability. Enzymes are large proteins, composed of a set of amino acids. The specific set of amino acids gives the enzymes a particular shape, size, and bio-chemical behavior. The active sites of the enzymes can bind to a particular analyte and catalyze a chemical reaction. The selectivity of the enzymatic reaction is achieved due to electrostatics, hydrogen-bonding, and other non-covalent interactions between the enzyme structure and the analyte of interest. A great advantage of enzymes lies in the fact that they are not altered during the chemical reaction, and this would allow for the

TABLE II. Comparison between different bio-recognition elements (enzymes, antibodies, aptamers and ion selective membranes) for EG-CNTFET-based bio-sensing applications, with a summary of advantages and limitations.

Bio-recognition element	Characteristics	Target analyte	CNT type/composite	Linear detection range	Ref.
Enzymes	Pros	Lactate	CNTs	10^{-3}–10^{6} nM	14
	–High sensitivity	Glucose	CNTs	10^{-3}–10^{5} nM	14
	–Commercially available	Acetylcholine	CNTs	10^{-3}–10^{6} nM	85
	Cons	Glutamate	SWCNTs/Pt NP	10^{-1}–10^{5} nM	87
	–Enzyme activity	Glucose	SWCNTs/PDDA	2×10^{6}–1×10^{7} nM	82
Antibodies	Pros	Lyme flagella	CNTs/diazonium salts	1–3000 ng/mL	52
	–High selectivity	Arginase	MWCNTs	30–100 ng/mL	35
	–Commercially available	PSA	SWCNTs	10^{-1}–10^{2} nM	73
	Cons	Aspergillus	SWCNTs	5×10^{-4}–1×10^{7} nM	78
	–Debye length limitation	Atrazine	SWCNTs	4.6×10^{-3}–4.6×10^{1} nM	34
Aptamers	Pros	IgE	CNTs	2.5×10^{-1}–1.6×10^{2} nM	56
	–High selectivity	Thrombin	CNTs	10^{-1}–1 nM	70
	–Detection within λ_D	K^+	CNTs	1×10^{-1}–1.1×10^{3} nM	26
	Cons	CatE	SWCNTs	0.1–1 ng/mL	69
	–Complicated synthesis	IL-6	CNTs	1×10^{-3}–1×10^{-2} nM	88
Ion-selective membranes	Pros	K^+ or Ca^{2+}	CNTs	10^{1}–10^{6} nM	59
	–Stable in harsh chemical environment	Na^+, K^+, Ca^{2+}, NH_4^+ and pH	CNTs	⋯	60
	Cons	pH	SWCNTs/PAA	2–12	77
	–Poor adhesion to semiconducting material	Ca^{2+}	CNTs/PVC	10^{3}–10^{8} nM	82
		K^+	SWCNTs/PDDA	10^{5}–10^{8} nM	86

fabrication of reusable sensors.[143] Their main drawback is the low stability that limits the biosensor shelf life.[144,145]

Antibodies consist of two heavy chains and two light chains of proteins, synthesized from animals. Each end of the antibody contains a paratope (analogous to a lock), which specifically binds to the epitope (analogous to a key) of the antigen (which represent the analyte).[146] The main advantage of using antibodies in bio-sensing is the fact that they are commercially available for a wide range of different analytes. In addition to their large employment, the main drawback is related to their bulky size that can lead to detection of the analyte outside the Debye length.[136]

The Debye length issue can be addressed through the use of aptamers, which are single-stranded oligonucleotides, synthesized *in vitro* using the systematic evolution of ligands by exponential enrichment (SELEX) process.[147,148] By varying the primary oligonucleotide sequences, high selectivity can be achieved, and this can be done for a wide range of analytes from proteins to small molecules.[148,149] The use of aptamers has gained popularity in electrochemical sensing due to their high selectivity and ability to overcome the Debye length limitation by undergoing target-specific conformational changes that occur in close proximity to sensing surfaces.[16,150] These conformational changes allow the detection of analytes even in high ionic strength solutions (i.e., solutions with very small λ_D), which is a critical challenge when using protein-based bio-recognition elements. Thus, integration of aptamers with optimized binding properties into EG-CNTFETs leads to highly sensitive and selective biosensors.[16,26,69] Moreover, aptamers are also characterized by a good stability in complex environments due their chemical nature.[151–154]

The main challenge for aptamers is the complicated synthesis procedure needed to isolate highly selective sequences able to undergo significant conformational rearrangements upon target recognition. Methods that employ advanced SELEX strategies to design structure-switching sequences have been reported. Details on the SELEX process can be found in the literature.[155–157]

While enzymes, antibodies, and aptamers have been used to detect bio-molecules and bio-markers,[3,14,73] the need to detect ions in several fields, such as environmental water analysis, medicine, chemical, and biological research, has led to the development of new synthetic sensing materials called ion-selective membranes.[59,77,83] Ion-selective membranes are synthesized by mixing a supporting material [e.g., poly(vinyl alcohol) (PVA)], which gives the structural properties to the membrane, a plasticizer, an ionophore, which is the sensing component of the membrane, and an anion or cation excluder component, which reduces the competitive coordination between the ionophore and the counter ions. Their working principle is based on the ion exchange, while the selectivity is achieved by the presence of the ionophore.[158] Synthetic recognition elements such as ion-selective membranes offer satisfactory selectivity and great stability in harsh chemical environments.[77] However, their adhesion to the semiconducting channel still remains challenging.[159]

C. The issue of nonspecific binding

To fabricate selective EG-CNTFET-based biosensors, the surface of the CNTs should be functionalized in such a way that would ensure specific binding with the analyte of interest, while preserving the electric properties of the nanotubes.[160]

The transduction mechanism in EG-CNTFETs is based on the presence of charges near the surface of the CNT channel (i.e., within the Debye length) that cause measurable current changes. Such biosensors are highly sensitive but not selective in terms of differentiating the bio-recognition binding events from nonspecific adsorption to both background molecules and the recognition elements themselves.[69,161] Therefore, in addition to choosing highly specific bio-recognition elements, an important matter to ensure specific binding is the insulation of the CNT channel. If not properly insulated, the CNT channel of the EG-CNTFET could be subject to modulated electrostatic gating, charge transfer, etc., due to nonspecific interactions with interfering analytes, leading to false positive results.

To minimize the nonspecific interactions, the sidewalls of bare nanotubes must be insulated. Several blocking reagents (insulating the CNT channel) are reported in the literature such as bovine serum albumin (BSA),[3,160] Tween-20[88] and ethanolamine.[69,79,150] Such blocking steps reduce nonspecific interactions and thus attribute the recorded current changes to the interaction between the bio-recognition element and the analyte of interest. In addition to surface blocking steps, to further reduce the non-specific binding one can do internal referencing (e.g., having a nonbinding element on the same device).[162]

Another approach that could be employed for the CNT channel encapsulation is the use of lipophilic membranes, as reported by Joshi *et al.*[163] Such treatments improve EG-CNTFET characteristics with the on–off ratio increased by over 2-fold, the hysteresis reduced by 10-fold, and the gate leakage current lowered by two orders of magnitude. Such improvements are the result of the insulation of the surface of CNTs by the lipophilic membrane, which does not allow ambient impurities to modulate the conduction of the nanotubes. The use of the lipophilic membrane, however, implies that no bio-recognition element can be attached on the surface of the CNTs: when such an approach is employed to insulate the CNT channel, only the functionalization of the gate can be then explored to achieve a selective response toward the analyte of interest.

V. BIOSENSOR EXAMPLES

In Secs. V A–V D, the working principle of EG-CNTFETs functionalized with enzymes (Sec. V A), antibodies (Sec. V B), aptamers (Sec. V C), and ion-selective membranes (Sec. V D) is briefly described and specific examples of biosensors are given.

A. Enzymatic sensors

The working mechanism of enzyme-modified EG-CNTFETs (called enzymatic sensors) is based on the catalytic reaction of the immobilized enzyme to oxidize/reduce the analyte of interest into a secondary product, leading to a variation of the I_{DS} current, as explained in Sec. II D.[3,14] In particular, the sensing mechanism of enzyme-based EG-CNTFETs is based on one of the following enzymatic reactions:

$$Reactant_1 + O_2 \rightarrow Product_1 + H_2O_2, \quad (8)$$

$$Reactant_1 + H_2O \rightarrow Product_1 + H^+, \quad (9)$$

where $Reactant_1$ is the analyte of the interest, while $Product_1$ is the primary product formed by enzymatic catalysis. In reaction 8, the secondary product (H_2O_2) is further oxidized into H^+ ions by applying the oxidation potential at the gate. In reaction 9, the secondary products are directly H^+ ions. In both cases, an increase in H^+ ions occurs leading to an increase in the number of positive charges in the electrolyte solution near the gate [due to the negative bias applied, see Fig. 2(b)]. This effect induces an increase in the negative charges near the CNT channel, thus an accumulation of positive charge carriers in the semiconducting channel, which is reflected in an increase in the absolute value of the I_{DS}.[85] The amount of H^+ ions produced will determine the change in the current, while being directly correlated with the amount of the analyte of interest.

A good description of the aforementioned mechanism in the case of EG-CNTFETs is reported by Lee and Cui, who showed flexible EG-CNTFETs functionalized with glucose oxidase for glucose detection.[82] In this case, a mixture of poly(diallyldimethylammonium chloride) (PDDA) and SWCNTs was deposited through dip-coating to form the semiconducting channel of the device [see Fig. 6(a-i)], while an external Ag/AgCl reference electrode was used as the gate electrode [see Fig. 6(a-ii)]. The EG-CNTFETs showed a real-time linear detection range between 2×10^6 to 1×10^7 nM as a result of oxidation of glucose into d-glucono-δ-lactone, followed by the hydrolysis of the latter to produce H_2O_2, which was finally oxidized under -1.5 V applied gate potential [see Fig. 6(a-iii)]. Interestingly, the same device worked also as a pH sensor without the enzyme immobilization with an absolute I_{DS} exponential increase with a pH decrease. In fact, the decrease in pH (i.e., the increase in H^+ concentration in the electrolyte) led to an increase in the absolute I_{DS}, as explained at the beginning of this section. Unfortunately, the authors did not show simultaneous measurement of pH and glucose, and it is therefore not clear how it is possible to differentiate the two signals.

As described in Sec. IV A, enzymatic EG-CNTFET biosensors can be realized employing diverse immobilization approaches, including the functionalization of the substrate as reported by Joshi *et al.*, who presented a flexible EG-CNTFET for the detection of glucose and lactate fabricated on PI.[14] The authors took advantage of the chemical properties of the PI and immobilized the enzymes (glucose oxidase and lactate oxidase) directly on the surface using the dicarboxylic acid—glutaric acid as a binder molecule: one end was used to bind to the nitrogen end of the PI surface, while the other carboxylic end was used to bind to the amine group of the enzyme. The devices showed a typical p-type behavior with an I_{ON}/I_{OFF} of about 260 A/A. After functionalization with lactate oxidase, the EG-CNTFET responded to lactate in a wide range of concentrations from 10^{-3} to 10^6 nM [see Fig. 6(b-i)] with sensitivity of 2.198 μA/decade [see Fig. 6(b-ii)], while the sensor functionalized with glucose oxidase showed a linear response for glucose in the range of 10^{-3} to 10^5 nM with sensitivity of 1.658 μA/decade.

A different approach was chosen by Bhatt *et al.*, who presented a planar EG-CNTFET fabricated on a flexible PI substrate for acetylcholine detection, employing enzymes to functionalize the planar gold gate electrode.[85] Alkanethiol chemistry was used to functionalize the planar gold gate electrode with the acetylcholinesterase enzymes, by means of 3-mercaptopropionic acid as a binder molecule. The immobilized enzyme catalyzed the hydrolysis of acetylcholine into choline

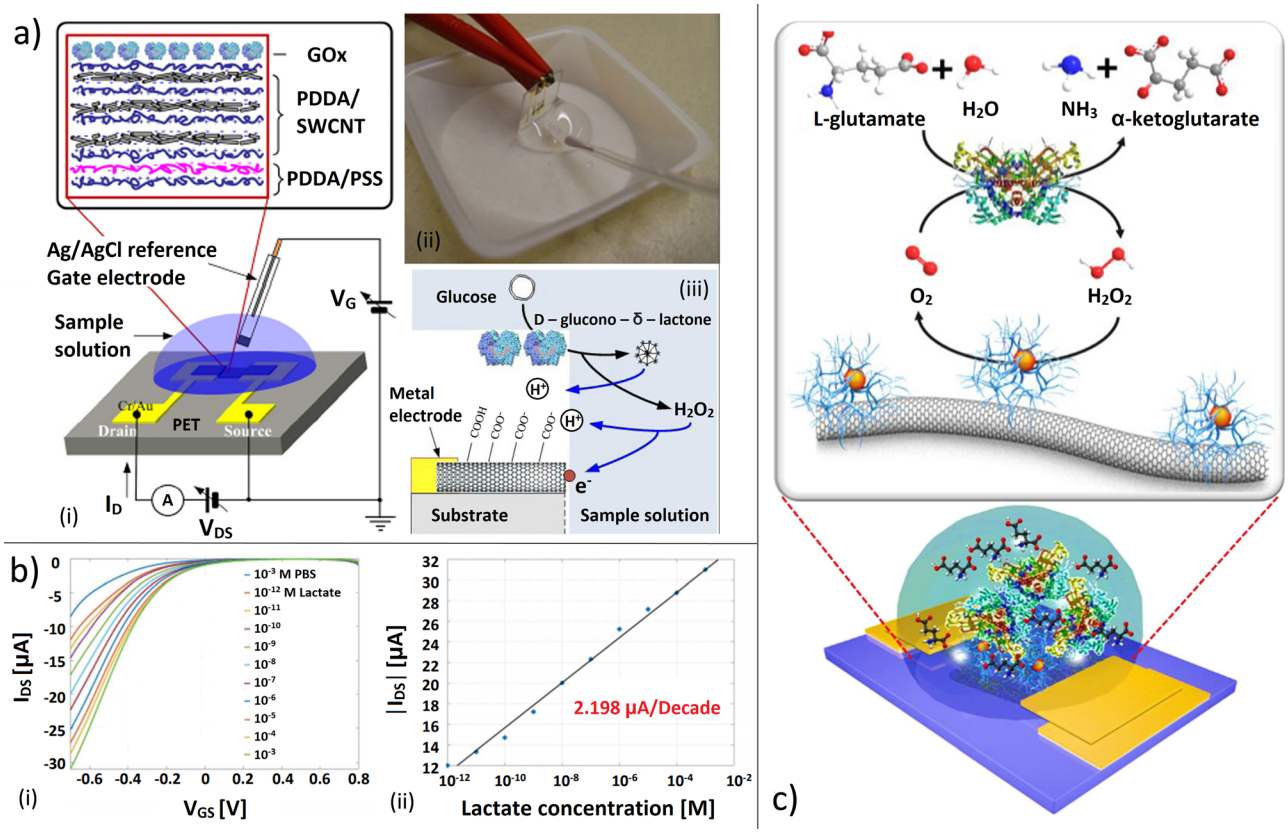

FIG. 6. Examples of EG-CNTFET-based enzymatic biosensors: (a) Glucose biosensor: (i) schematic diagram of EG-CNTFET, based on deposition of poly(diallyldimethylammonium chloride) (PDDA) and SWCNTs, functionalized with glucose oxidase—for selective glucose detection; (ii) a real picture of the experimental setup in which an external Ag/AgCl reference electrode is used as gate electrode for the fabricated EG-CNTFET; (iii) proposed sensing mechanism: the oxidation of glucose to d-glucono-δ-lactone and H_2O_2 is catalyzed by the glucose oxidase, followed by the hydrolysis of d-glucono-δ-lactone and the electrooxidation of H_2O_2 to produce hydrogen ions. Reproduced with permission from Lee and Cui "Low-cost, transparent, and flexible single-walled carbon nanotube nanocomposite based ion-sensitive field-effect transistors for pH/glucose sensing," Biosens. Bioelectron. **25**, 2259–2264 (2010).[82] Copyright 2010 Elsevier. (b) Lactate biosensor (i) response of flexible EG-CNTFET functionalized with lactate oxidase to different lactate concentrations, (ii) calibration curve for lactate biosensor: drain current vs lactate concentration. Reproduced with permission from Joshi *et al.*, "Flexible lactate and glucose sensors using electrolyte-gated carbon nanotube field effect transistor for non-invasive real-time monitoring," IEEE Sens. J. **17**, 4315–4321 (2017).[14] Copyright 2017 IEEE. (c) Glutamate biosensor—proposed sensing mechanism: the production of H_2O_2 from glutamate is catalyzed by glutamate oxidase, followed by catalytic decomposition of H_2O_2 to produce oxygen species. Reproduced with permission from Lee *et al.*, "Electrochemical functionalization of single-walled carbon nanotubes with amine-terminated dendrimers encapsulating pt nanoparticles: Toward facile field-effect transistor-based sensing platforms," Sens. Actuators, B **275**, 367–372 (2018).[87] Copyright 2018 Elsevier.

and acetic acid, releasing H^+ ions into the electrolyte solution. With increasing concentration of the acetylcholine in the electrolyte, an increase in the H^+ ions in the electrolyte surface near the gate was induced, ultimately leading to an increase in the absolute value of the I_{DS} according to the mechanism described at the beginning of this section. Transfer curves were recorded with a fixed V_{DS} at -0.2 V, while sweeping V_{GS} from $+0.8$ to -0.8 V for different concentrations of acetylcholine. The sensor showed a real-time response for acetylcholine detection in the concentration range of 10^{-3} to 10^{6} nM, with the calculated sensitivity of 5.6855 μA/decade.

Enzymes are also used to directly functionalize the semiconducting CNT channel. For instance, Dudina *et al.* reported a sensing platform realized using a CMOS chip.[3] The CMOS implementation (i.e., the combination of n-type and p-type elements for the realization of circuital elements) was used to realize the amplification/readout circuitry very close to the EG-CNTFET array used as sensing element. The EG-CNTFETs were functionalized for glutamate detection, by covalently attachment of the enzyme glutamate oxidase to the carboxylated CNTs. The working principle of the sensor was based on enzymatic oxidation of glutamate, which produced H_2O_2. The EG-CNTFET array demonstrated a real-time response for glutamate with a linear detection range between 2.5×10^5 and 5×10^5 nM achieved by oxidizing the H_2O_2 (product of glutamate oxidization by the enzyme) with a potential of -0.65 V applied to the gate.

In addition to the different sites of functionalization (substrate, gate, semiconductor), the enzymatic EG-CNTFET biosensors can be realized using different FET configuration as explained in Sec. II A. For example, Barik *et al.* reported a dual-gated FET, based on CNTs doped with polyethylene imine channel, Ag/AgCl top gate and indium tin oxide as a back gated for acetylcholine detection.[120] In this case, the

detection of acetylcholine is based on the hydrolysis reaction catalyzed by acetylcholine esterase to produce acetic acid and choline. The sensor showed a linear detection range 1×10^4 to 2×10^5 nM and sensitivity of 1.25 V/decade for acetylcholine detection.

An interesting functionalization approach of the CNTs involves the use of metal nanoparticles before the immobilization of the enzymes, as presented by Lee *et al.* The authors proposed an EG-CNTFET based on electrochemical functionalization of CNTs with amine-terminated dendrimers encapsulating platinum nanoparticles (Pt DENs) for glutamate detection.[87] The device fabrication started with the adsorption of CNT suspension (0.1 mg/mL in o-dichlorobenzene) on the SiO_2 surface treated with octadecyltrichlorosilane, followed by standard photolithography to pattern the source and drain electrodes. Afterward, cyclic voltammetry was used to functionalize the CNT film with Pt DENs. Finally, enzyme glutamate oxidase was absorbed on the CNT-Pt DENs channel. Integration of the Pt DENs into the CNT film enhanced the electrocatalytic activity of the sensors; furthermore, the amine groups grafted on Pt DENs offer a new interesting approach for immobilization of the bio-recognition element. The glutamate oxidase enzyme catalyzes the oxidation of glutamate, leading to the release of electrochemically active H_2O_2 as a secondary product of the enzymatic reaction [see Fig. 6(c)]. Catalytic decomposition of H_2O_2 led to an increase in the absolute value of the I_{DS}, due to the increased concentration of H^+ in proximity of the semiconducting channel. The sensor showed a wide dynamic range of detection from 10^{-1} to 10^5 nM with calculated limit of detection as low as 0.092 nM. The sensing ability of the device was demonstrated on real samples (rice soups) without any pretreatment, showing acceptable sensitivity in the range of 10^{-1} to 10^5 nM.

In general, the demonstration of the sensing properties of enzymatic EG-CNTFET-based biosensors in real applications is still missing in the literature and limited *in vivo* applications are reported. Among these, we can cite the work of Lee *et al.*, who reported EG-CNTFETs for glutamate detection.[80] The sensor fabrication started from a glass capillary tube which was dipped into SWCNTs dispersion (in 1,2-dichlorobenzene), followed by thermal evaporation of source and drain electrodes (10 nm of Ti and 30 nm of Au) and use of a Pt wire as a gate electrode. Glutamate oxidase was immobilized on the CNT channel using PBASE as a linker molecule. The sensor showed a real time linear detection range between 300 to 15 000 nM, with the coefficient of determination as high as 0.99. Furthermore, the sensing capability of the sensor was demonstrated *in vivo* for monitoring glutamate released during intra- and post-ischemic periods on 11 vessel occlusion rat model.

B. Immunosensors

Antibody-modified biosensors (called immunosensors) are based on the specific antigen (Ag)–antibody (Ab) interaction, which has attracted significant interest in the realization of EG-CNTFET-based biosensors due to its high selectivity. An antibody typically recognizes only one specific antigen, forming an Ab–Ag immunocomplex. This reaction is highly selective but sometimes cross-reactivity is possible.[164] The binding affinity between an Ab and an Ag (for a noncompetitive reaction) can generally be expressed by the following formula:

$$K = \frac{[Ab - Ag]}{[Ab][Ag]}, \tag{10}$$

where K is the equilibrium constant, [Ab-Ag] is the concentration of the immunocomplex formed between Ab and its specific Ag, and [Ab] and [Ag] are the concentrations of the Ab and the Ag, respectively (expressed in mol L^{-1}). Typical values of K range from 10^6 to 10^{12} L mol^{-1}. For K values $\geq 10^8$ L mol^{-1}, antibodies will typically exhibit low cross-reactivity and therefore lead to high selectivity.[164]

When antibodies are used in EG-CNTFET-based biosensors, the sensing mechanism is based on the immunoreaction formation between the target antigens with the antibodies immobilized on the CNT channel, causing a change in the surface charges[58,72] and thereby a change of the I_{DS}. In this regard, Teker suggested that the change in the I_{DS} resulting from the attachment of the antibodies (anti-insulin-like growth factor 1 antibodies) is related to the capability of the amine group of the antibodies to donate electrons to the CNTs.[58] When breast cancer cells (BT474 or MCF7) were injected into the device, a significant increase in the I_{DS} was observed. The authors explained this increase due to the electron transfer from the CNTs to the immunocomplex (holes density increases).

A different behavior has been reported by Palaniappan *et al.*[73] They realized an EG-CNTFET-based immunosensor based on partially aligned SWCNTs grown on quartz substrates for the detection of prostate-specific antigen (PSA), where anti-prostate antibodies were immobilized on the SWCNTs using PBASE ester as a binder molecule [see Fig. 7(a-i)]. First, the authors compared the transfer characteristics of EG-CNTFETs fabricated using random and aligned SWCNTs networks, demonstrating the superior performance (i.e., higher absolute value of I_{DS}) of the device fabricated using the latter [see Fig. 7(a-ii)]. Upon the injection of different concentrations of PSA, a decrease in the measured absolute I_{DS} was observed [see Fig. 7(a-iii)]. Since PSA has positive surface charge potential, its attachment to the anti-prostate antibodies caused a decrease in the absolute value of the I_{DS} due to electrostatic interaction between positively charged analytes and SWCNTs (i.e., the positive charge potential of the PSA caused a depletion of holes in the semiconducting channel, hence less current). The sensing capability of the device toward PSA was demonstrated in the range of 1×10^{-1} to 1×10^2 nM, with a calculated LOD as low as 3×10^{-2} nM. The group has applied the same concept for the detection of the food toxin Clostridium perfringens, achieving an LOD as low as 2 nM.[74]

As explained in Sec. II D, good sensitivity can be obtained only if the immunoreaction happens within the λ_D.[42] Therefore, a challenging aspect for EG-CNTFET-based immunosensors is the bulky size of antibodies (10–12 nm),[79] which is larger than the λ_D of physiological solutions (<1 nm). As already stated, to increase the λ_D, some authors use diluted PBS. For example, Jin *et al.* reported EG-CNTFETs based on acid treated SWCNTs functionalized with antibodies for rapid and selective detection of Aspergillus species.[78] The authors used a low PBS concentration (0.15× PBS, i.e., 6.7 times diluted with respect to 1× PBS) characterized by a λ_D of around 9 nm. As the antibodies used in this study have a height of around 3 nm, the immunoreaction happened within the λ_D. The sensor showed a real-time response upon successive injections of Aspergillus [see Fig. 7(b-ii)], and a linear detection range between 5×10^{-4} to 1×10^7 ng/mL [see Fig. 7(b-iii)], with an estimated detection limit of 1×10^{-4} ng/mL.

To address the Debye length issue while maintaining undiluted PBS concentration, Kim *et al.* reported EG-CNTFETs functionalized by three different bio-receptors: complete anti-immunoglobulin

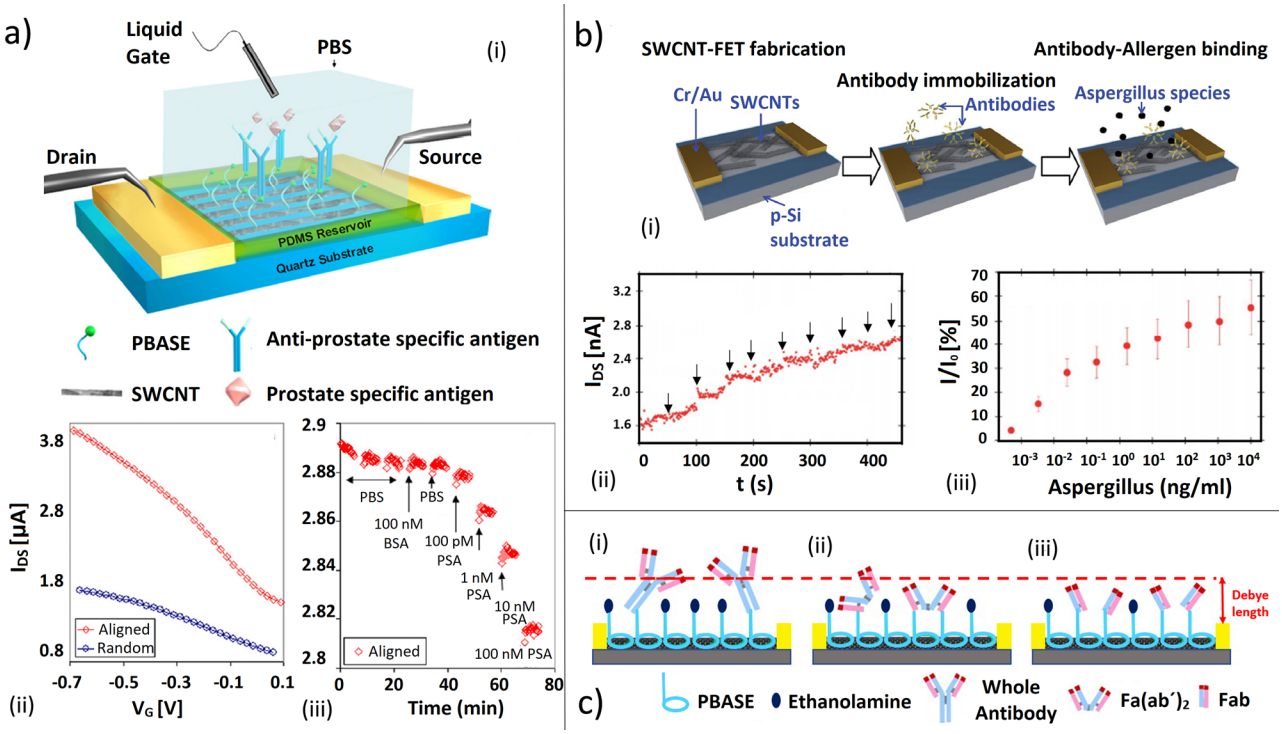

FIG. 7. Examples of EG-CNTFET-based immunosensors: (a) Prostate-specific antigen (PSA) biosensor, (i) schematic of biosensor on quartz substrate for real-time detection of PSA, (ii) the EG-CNTFET transfer characteristics for the device with random (blue) and aligned (red) CNT network, (iii) real-time measurement of different PSA concentrations at −300 mV fixed gate voltage. Reproduced with permission from Palaniappan *et al.*, "Aligned carbon nanotubes on quartz substrate for liquid gated biosensing," Biosens. Bioelectron. **25**, 1989–1993 (2010).[73] Copyright 2010 Elsevier. (b) Aspergillus biosensor, (i) schematic diagram describing step by step antibody (anti-Aspergillus) immobilization and antibody-allergen binding, (ii) real-time response to successive additions (indicated by the arrows) of Aspergillus, (iii) corresponding calibration curve: drain current vs Aspergillus concentrations (from 10^{-3} to 10^{4} ng/mL). Reproduced with permission from Jin *et al.*, "Real-time selective monitoring of allergenic aspergillus molds using pentameric antibody-immobilized single-walled carbon nanotube-field effect transistors," RSC Adv. **5**, 15728–15735 (2015).[78] Copyright 2015 Royal Society of Chemistry. (c) Immunoglobulin biosensor, schematic of functionalization of the semiconducting CNT channel with three different bio-receptors: (i) whole antibody (height 10–12 nm), (ii) F(ab')$_2$ fragments (height 7 nm), and (iii) Fab fragments (height 3–5 nm). Reproduced with permission from Kim *et al.*, "Ultrasensitive carbon nanotube-based biosensors using antibody-binding fragments," Anal. Biochem. **381**, 193–198 (2008).[79] Copyright 2008 Elsevier.

G (anti-IgG) antibodies with size of 10–12 nm [see Fig. 7(c-i)], F(ab')$_2$ fragments of anti-IgG with a height of approximately 7 nm [see Fig. 7(c-ii)], and only the Fab fragments of anti-IgG with the height of 3–5 nm for IgG detection [see Fig. 7(c-iii)].[79] The authors tested the device for different IgG concentrations, and observed a decrease in the absolute value of I_{DS} after the injection of the analyte, accordingly with the IgG being positively charged. The device with complete antibodies was not able to detect IgG concentration lower than 100 ng/mL, while the device with F(ab')$_2$ fragment was able to detect 10 ng/mL, and the device with immobilized Fab fragments was able to detect IgG concentration as low as 10^{-3} ng/mL. The authors concluded that the enhancement in the immunosensor device response was due to the use of antibodies with a size that enabled the immunoreaction to take place within the Debye length.

C. Aptasensors

Aptamers are artificial single-stranded oligonucleotides that have gained interest for bio-sensing vs protein-based recognition elements due to their high selectivity and tunable stability.[165] Compared to enzymes and antibodies, aptamers are smaller in size,[16,79] which facilitates sensitive bio-molecule detection within the λ_D in physiological conditions.[56,57,166] Signal transduction upon aptamer target recognition at the surface of the EG-FET channel has been hypothesized to arise from two main mechanisms.

The first mechanism, more common for small-molecule detection, involves structural rearrangements of the negatively charged aptamer phosphodiester backbone upon target capture.[167–169] Aptamer conformational change drives surface charge rearrangement at the surface of the semiconducting channel, which enables the detection of even neutral small-molecule targets such as glucose.[16] As aptamers are highly negatively charged molecules, changes in the channel current flow are measurable even for low analyte concentrations.[26]

An example of sensing based on the structural rearrangement can be found in the work of Zheng *et al.*, who presented flexible EG-CNTFETs functionalized with conformationally changing 21-mer aptamers for potassium ion (K^+) detection.[26] Aptamers were attached to the CNTs via $\pi - \pi$ interactions of PBASE linker [see Fig. 8(a-i)]. Real-time sensing upon addition of K^+ to the aptamer-modified

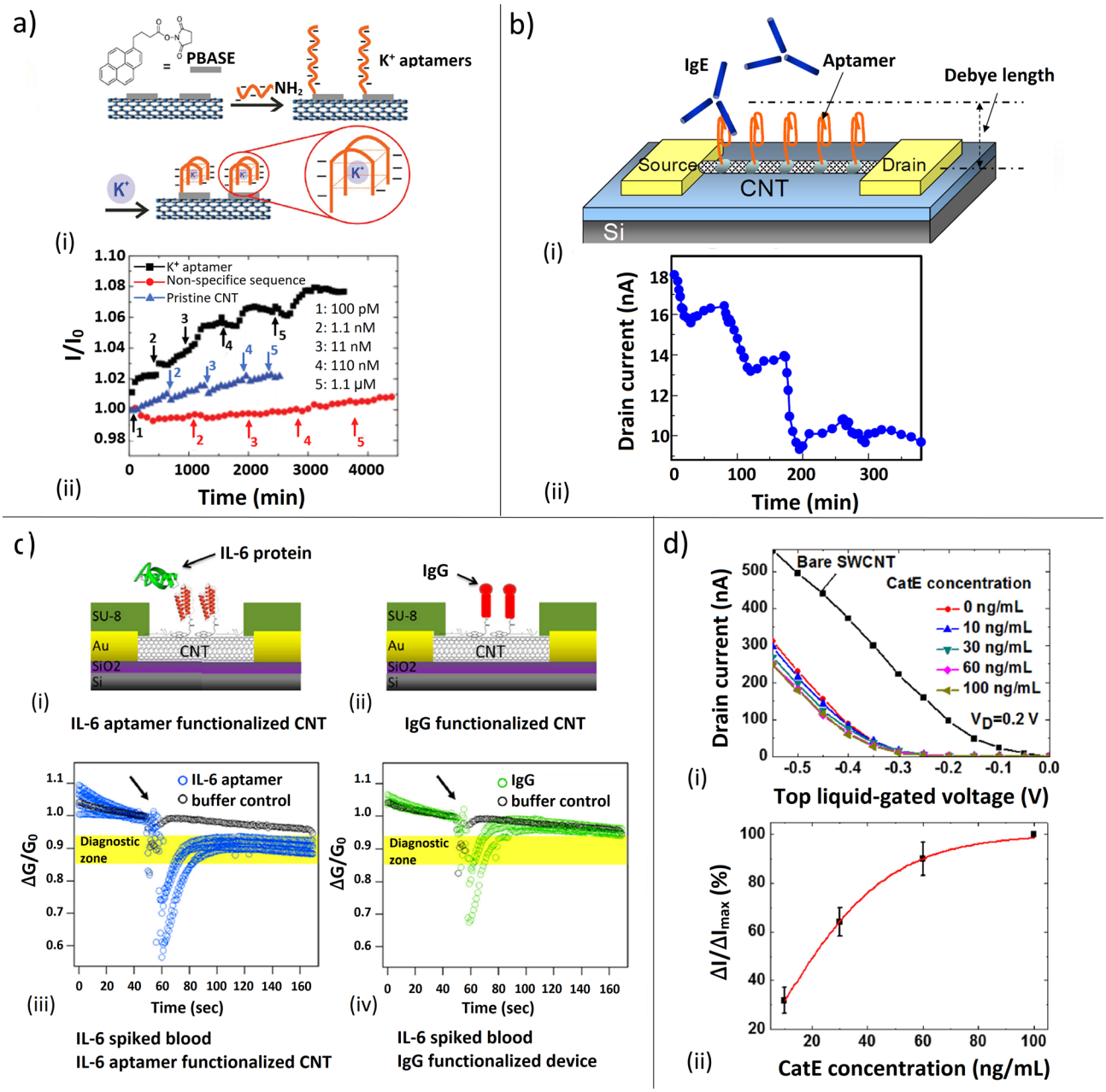

FIG. 8. Examples of EG-CNTFET-based aptasensors: (a) K^+ biosensor, (i) functionalization of CNT channel with K^+ aptamers using PBASE linker molecule, sensing mechanism: K^+ aptamers folding after K^+ addition, (ii) real-time response toward successive additions of K^+. Reproduced with permission from Zheng *et al.*, "Electrostatic gating in carbon nanotube aptasensors," Nanoscale **8**, 13659–13668 (2016).[26] Copyright 2016 Royal Society of Chemistry. (b) Immunoglobulin E (IgE) biosensor, (i) detection within Debye length using aptamers, (ii) real-time response upon successive additions of IgE. Reproduced with permission from Mahehashi *et al.*, "Aptamer-based label-free immunosensors using carbon nanotube field-effect transistors," Electroanalysis **21**, 1285–1290 (2009).[56] Copyright 2009 IEEE. (c) Interleukin-6 (IL-6) protein biosensor, (i) CNT channel functionalization with IL-6 peptide aptamers using PBASE linker molecule and (ii) immunoglobulin G (IgG) nonspecific aptamer (control device), (iii) real-time response of EG-CNTFET functionalized with IL-6 aptamer in blood samples. The device showed 8%–13% drop in the absolute value of the current upon addition of 10 pg/mL of IL-6 protein, (iv) real-time response of device functionalized with IgG aptamer. No significant change in the current was observed. Reproduced with permission from Khosravi *et al.*, "Ultrasensitive label-free sensing of IL-6 based on PASE functionalized carbon nanotube micro-arrays with RNA-aptamers as molecular recognition elements," Biosensors **7**, 17 (2017).[88] Copyright 2017 Authors, licensed under a Creative Commons Attribution (CC BY 4.0) license. (d) Cathepsin (CatE) biosensor, (i) transfer characteristics of the EG-CNTFET functionalized with the peptide aptamers for different CatE concentrations in 10-fold diluted human serum, (ii) CatE concentrations vs the normalization decrease in "on" current. Reproduced with permission from Tung *et al.*, "Peptide aptamer-modified single-walled carbon nanotube-based transistors for high-performance biosensors," Sci. Rep. **7**, 1–9 (2017).[69] Copyright 2017 Authors, licensed under a Creative Commons Attribution (CC BY 4.0) license.

EG-CNTFET was recorded by applying a fixed V_{DS} of 100 mV and V_{GS} of 0 V. An increase in the absolute value of the I_{DS} was observed upon the addition of K^+ (from 1×10^{-3} to 1×10^{3} nM), while devices without the aptamer functionalization or modified with a nonspecific sequence showed no change in the current response [see Fig. 8(a-ii)]. The authors hypothesized that aptamers that folded upon target recognition increased the negative charge density near the p-type CNT channel, inducing an increase in the concentration of the holes, and hence an increase in the drain current.

The second mechanism involves the detection of charged targets upon aptamer binding. Thrombin, a popular target protein for aptamer-FET platforms, is positively charged at low pH (lower than 7).[170] Thus, thrombin binding to aptamers has been proposed to effectively screen the negative charges of the oligonucleotide, while also bringing new sources of positive charge in close proximity of the CNT channel.

Alternatively, Pacios *et al.* reported thrombin detection using aptamer-based EG-CNTFETs in an environment in which thrombin was slightly negatively charged (at pH 7.9).[70] After the injection of thrombin, an increase in the absolute value of the I_{DS} was observed. The increase in the positive charge carriers in the CNT channel (i.e., in the I_{DS}) was considered by the authors as a consequence of the more negatively charged species brought closer to the λ_D. The device was characterized in 0.05× PBS, a diluted environment to detect the charges of the large thrombin target molecule approaching the EG-CNTFET surface. Using this approach (albeit, in a non-physiological environment), low concentrations of thrombin (in the range of 1×10^{-1} to 1 nM) were measured with a calculated LOD of 2×10^{-2} nM.

Despite the increasing employment of aptamers in EG-FET-based biosensors, and, in general, in electronic biosensors, the sensing mechanism is still not well understood. Outside of the aforementioned examples, some authors merely reported the measurable changes in the electrical properties of the device in the presence of the specific analytes without an explanation of the sensing mechanism.[56,69,88]

For instance, Maehashi *et al.* reported an aptamer-based EG-CNTFET for immunoglobulin E (IgE) detection [see Fig. 8(b-i)].[56] The IgE aptamers were covalently attached to the CNT channel using PBASE as a linker molecule. Real-time sensing of IgE in the range 2.5×10^{-1} to 1.6×10^{2} nM was conducted [see Fig. 8(b-ii)].

Alternatively, Khosravi *et al.* presented a EG-CNTFET microarray functionalized with aptamers targeting interleukin-6 (IL-6) for rapid detection of the IL-6 cancer biomarker [see Fig. 8(c-i)].[88] To demonstrate the selectivity of the device, the authors functionalized the device with nonspecific control sequences [see Fig. 8(c-ii)]. The device functionalized with specific IL-6 aptamers showed a linear response in the range 1×10^{-3} to 1×10^{-1} ng/mL. Furthermore, the sensing capability of the devices was demonstrated in blood samples, where aptamer-functionalized devices showed a 8%–13% drop in the current upon addition of 10 pg/mL of the IL-6 protein [see Fig. 8(c-iii)], while the device functionalized with nonspecific IgG displaced a reduced change in current [see Fig. 8(c-iv)]. The observed response for the control is likely due to the inevitable nonspecific binding in complex media.[162]

In both of these reports, the authors asserted that the decrease in absolute value of the I_{DS} was associated with the fact that positively charged molecules came close to/within the λ_D, inducing an increase in the density of the negative charge in the EG-CNTFET channel. Nevertheless, the authors did not take into account the effect of the negatively charged aptamers in the conductance changes.

Similarly, the involvement of the recognition element in the mechanism of signal transduction was omitted in the work of Tung *et al.*, who presented sensitive EG-CNTFETs for the detection of Cathepsin E (CatE), a cancer biomarker, using peptide aptamers.[69] Peptide aptamers are small (typically 5–20 amino acid residues long) proteins selected to bind to specific sites of target molecules.[171] The authors performed a systematic investigation on the effect of the CNT bio-functionalization using the I_{DS}-V_{GS} curve. To immobilize the CatE peptide aptamer, PBASE was used as a linker. The results showed that the absolute value of the I_{DS} decreases with the increase in the PBASE concentration from 3 to 50 mM. The authors considered this behavior due to the charge transfer induced by $\pi - \pi$ interactions between the PBASE and SWCNTs, leading to the current reduction. Similar behavior was also observed by varying the peptide aptamer concentration (in the range from 1 to 120 μM).

As the peptide aptamer exhibits a positive charge in PBS at pH 4, its presence in proximity of the CNT channel led to a decrease in the concentration of the holes and hence decrease in absolute value the I_{DS}. Addition of CatE (from 0.1 to 1 ng/mL) resulted in a further decrease in the absolute values of the I_{DS}, which was hypothesized to be caused by the reduction of holes in the CNT channel as a result of positively charged CatE binding [see Fig. 8(d-i)]. The sensing capability of the device was also demonstrated in human serum for CatE concentrations in the range of 10 to 60 ng/mL [see Fig. 8(d-ii), where ΔI_{max} is the decrease in I_{ON} in the saturation regime]. A LOD as low as 10 ng/mL was achieved, which was three orders of magnitude lower than what is measured by conventional enzyme-linked immunosorbent assays (ELISA).[69] However, despite these promising measurements in blood samples, when describing the sensor mechanism, the authors disregard the possible conformational changes that the aptamer may undergo and how that phenomenon in combination with the charged target recognition would affect the I_{DS}.

To this end, it is critical to conduct complementary investigations into aptamer conformational changes using fluorescence-based, spectroscopic (e.g., circular dichroism, surface-enhanced Raman, impedance), or optical methods.[16,172] Insight into the sensing mechanisms will lead to optimization of these platforms for specific targets (e.g., detection of weakly charged or non-charged species) and sensing environments (e.g., high ionic strength physiological environments with small λ_D for detection).

D. Ion-selective membrane sensors

EG-CNTFETs based on ion-selective membranes are widely used for the measurement of ion concentrations,[81,173] due to their higher stability in harsh chemical environments, compared to the previously mentioned biological recognition elements (enzymes, antibodies, and aptamers). Indeed, the synthetic membranes can limit the direct contact between the device and the electrolytic solution, allowing the flow of only the target ions due to the presence of the ionophore. In the presence of an ion-selective membrane, a change of the analyte concentration causes a variation of the potential at the membrane interface, which can induce a change in the EG-CNTFET characteristics (e.g., V_{TH} or I_{DS}).[77]

EG-CNTFET-based biosensors functionalized with ion-selective membranes are often used to detect K^+, Ca^{2+}, and Cl^- ions. For

instance, Melzer *et al.* presented an EG-CNTFET for selective and sensitive detection of all these ions by functionalizing the gate electrode (Pt wire) with different poly(vinyl chloride) (PVC)-based ion-selective membranes [see Fig. 9(a-i)].[83] For K^+ quantification, the Pt gate was modified with a PVC-based membrane containing K^+ ionophore to ensure selectivity, and transfer curves for different K^+ ion concentrations were recorded. A shift toward positive voltages of the transfer curve was noticed with an increase in K^+ concentrations. To quantify the shift, the V_{TH} was extracted from the transfer curve and a linear response was found in the range of 10^2 to 10^8 nM of K^+ by plotting the V_{TH} vs the logarithm of the ion activity. The same concept was used to detect Ca^{2+} and Cl^-. In those cases, the Pt gate was functionalized with a PVC-based membrane containing Ca^{2+} ionophore and a PVC-based membrane containing Cl^- ionophore, respectively. The biosensors for Ca^{2+} showed a linear response in the range of 10^3 to 10^8 nM [see Fig. 9(a-ii)], while the biosensor for Cl^- detection showed a linear response in the range of 10^4 to 10^8 nM.

From the same authors, a similar example of flexible EG-CNTFETs modified with PVC-based ion-selective membranes was reported for K^+ or Ca^{2+} detection, but this time the membrane was directly drop-cast on top of the semiconducting CNT channel.[59] The sensor responses were tested in a physiologically relevant concentration range in the presence of different interfering ions. The response of EG-CNTFETs modified with K^+-selective membranes was demonstrated in the range of 10^1 to 10^8 nM K^+ solution diluted in 150 mM Na^+ or Ca^{2+} interfering ion. The sensor showed a linear response down to 10^2 nM for Na^+ and 10^3 nM for Ca^{2+}, respectively. The response of the EG-CNTFET modified with the Ca^{2+}-selective membrane was demonstrated in the range of 10^1 to 10^8 nM Ca^{2+} solution diluted in 150 mM Na^+- or Mg^{2+}-interfering ions. The biosensor showed a linear response down to 10^5 nM for Na^+ and 10^4 nM for Mg^{2+}, respectively. These EG-CNTFET-based biosensors represent an important step in the fields of biomedical diagnostics or water quality control. A good proof of this is the fact that this work was further expanded through the development of an array with a planar gate able to measure all the reported ions.[60] The biosensor response of the array was in good agreement with ion concentrations reported in the label of the water employed for the tests by the manufacturer.

An interesting example of EG-CNTFET array was presented by the same group.[61] The array consisted of two modified EG-CNTFETs with one shared planar gate electrode modified by drop-casting MWCNTs and functionalized with urease enzymes. The channels of the two EG-CNTFETs were functionalized with a NH_4^+-selective and an H^+-selective membrane, respectively [see Fig. 9(b-i)]. The urea detection was based on the hydrolyzation reaction catalyzed by urease; the products of this reaction, NH_4^+ and H^+ cations, were then detected by the ion-selective membranes. The array was tested for urea detection in the concentration range from 10^4 to 10^8 nM, in 0.01× PBS [see Fig. 9(b-ii)] and highly concentrated 2× PBS [see Fig. 9(b-iii)]. The NH_4^+-selective EG-CNTFET had a 1×10^5 nM LOD, while the H^+-selective EG-CNTFET showed a linear response in the physiological pH range 7–9. Employing a H^+-selective EG-CNTFET in the array would allow simultaneous pH monitoring, hence the possibility to real-time compensate for any change in the pH value of the electrolyte.

Most of the proposed ion-selective membranes, comprised the above cited works, use PVC as supporting material for the membrane realization, because of its low toxicity and chemical inertness. However, conducting polymers such as polypyrrole, polyaniline, or polythiophene are used as well, as they constitute a well-studied class of materials.[174]

In this direction, Gou *et al.* presented an EG-CNTFET for pH detection based on an ion-selective membrane made of conductive polymers.[77] The authors employed oxidized SWCNTs for the semiconducting channel coated with electrodeposited poly(1-aminoanthracene) (PAA) conductive film. The device response was tested over a pH range from 2 to 12. With the increase in the pH, the transfer curve was shifted to more positive gate voltages [see Fig. 9(c-i)]. The authors explained this shift due to more negative charge generation on the surface of the SWCNTs due to the deprotonation of carboxylic groups on the oxidized SWCNTs. Therefore, increasing the negative charge in proximity of the SWCNT channel caused an accumulation of positive carriers, hence yielding a shift in the threshold voltage. In this respect, the charge accumulated on the surface of the semiconducting channel directly affected the gating effect coming from the applied V_{GS}. A real-time pH measurement under constant −0.2 V gate voltage was demonstrated as well [see Fig. 9(c-ii)]. Furthermore, the authors demonstrated the implementation of this device into a wirelessly powered radio frequency identification (RFID) tag prototype. Wireless readings were performed on a tissue phantom mimicking the properties of human skin, suggesting the possible use of the device for *in vivo* monitoring.

Stelmach *et al.* proposed an EG-CNTFET-based biosensor for K^+ detection, functionalizing the planar gold gate electrode with polypyrrole nanoparticles dispersed in PVC-based ion-selective membranes.[86] The aim was to improve the EG-CNTFET characteristics, in order to obtain a more stable signal compared to PVC-bare based ion-selective membranes. The response of the sensor was tested in different concentrations of K^+ solution ranging from 10^4 to 10^8 nM. A linear response between the I_{DS} at a fixed voltage and the logarithm of K^+ concentration was found in the range of 10^5 to 10^8 nM. The author addressed this behavior due to the ability of the conducting polymer (in contact with the electrolyte solution) to be reduced or oxidized under the influence of the applied potential (in contrast to ion-selective membranes, which are usually chemically inert). This effect results in corresponding positive or negative charge injection into the CNT channel, leading to changes in the absolute value of the I_{DS}.

VI. CONCLUSIONS—PRESENT ISSUES AND CHALLENGES

The development of next-generation electronic biosensors with engineered functionalities and unobtrusive integration into every type of substrates (from rigid to flexible and biocompatible) will push toward the improvement of real-time digital monitoring (the Internet of Things philosophy) and will have positive economic implications. In this perspective, CNTFET-based, and, in particular, EG-CNTFET-based biosensors, enable versatile applications in several fields. A reliable integration of such technologies in suitable devices could significantly improve the monitoring of environmental conditions, health of humans, animals, and plants.

In this review, we reported in detail the most important achievements in the development and application of EG-CNTFET-based biosensors. The possibility to functionalize the CNTs following different strategies and using different surface chemistries enables a high degree

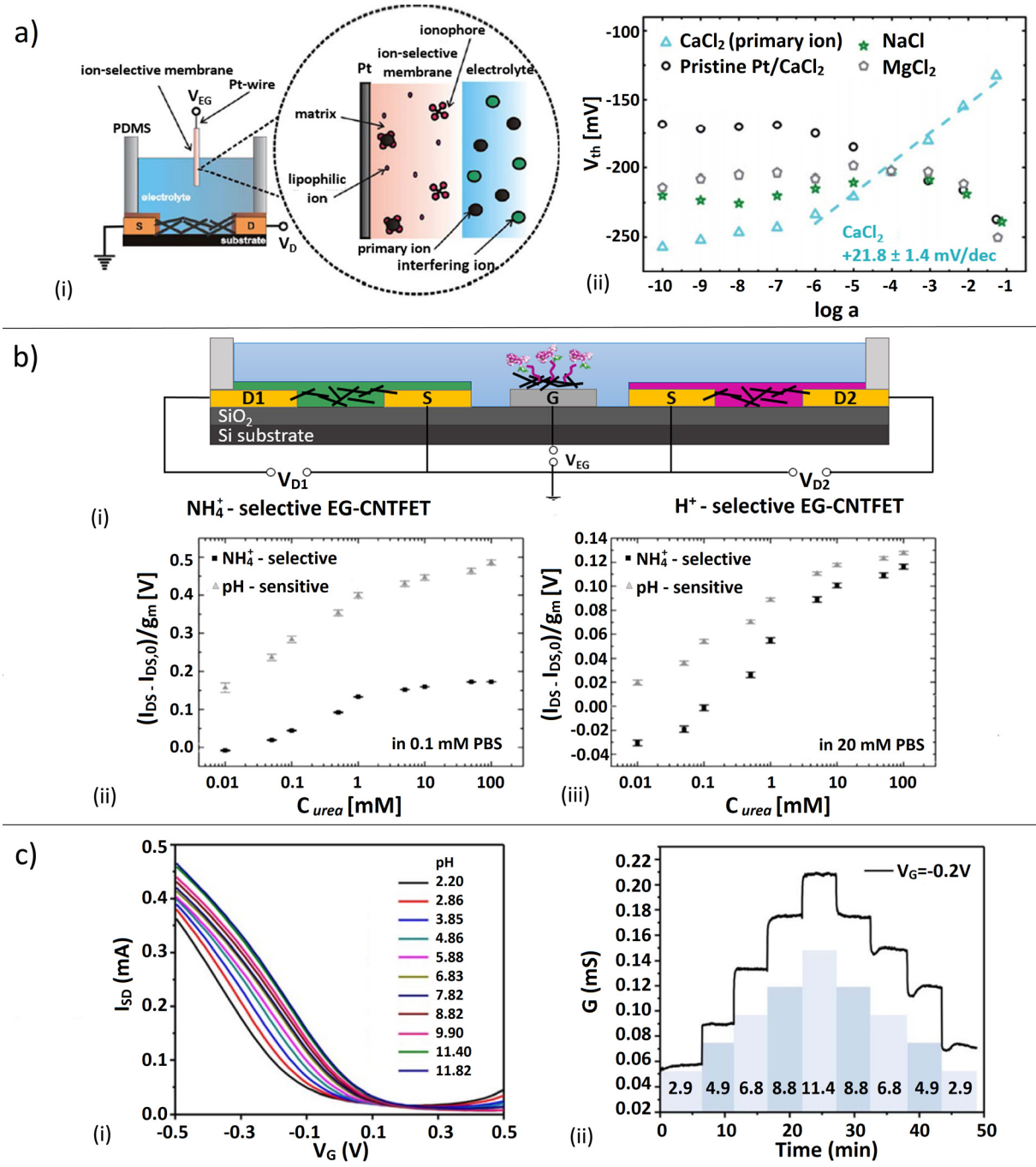

FIG. 9. Examples of EG-CNTFET-based ion-selective membrane sensors: (a) Ca^{2+} sensor, (i) device schematic, with emphasis on the functionalization for the gate electrode (platinum wire): the PVC-based ion-selective membrane allows the passage of the primary ions while blocking the interfering ions, thanks to the presence of the ionophore (ii) selective response of the EG-CNTFET toward Ca^{2+}. Reproduced with permission from Melzer *et al.*, "Selective ion-sensing with membrane-functionalized electrolyte-gated carbon nanotube field-effect transistors," Analyst **139**, 4947–4954 (2014).[83] Copyright 2014 Royal Society of Chemistry. (b) NH_4^+ and pH biosensor array, (i) schematic of the array composed of an NH_4^+ selective EG-CNTFET and a H^+ selective EG-CNTFET with a common planar gate electrode functionalized with urease enzyme, for urea and pH detection; (ii) selective response in diluted 0.1 mM (0.01×) PBS; and (iii) selective response in highly concentrated 20 mM (2×) PBS. Reproduced with permission from Melzer *et al.*, "Enzyme assays using sensor arrays based on ion-selective carbon nanotube field-effect transistors," Biosens. Bioelectron. **84**, 7–14 (2016).[61] Copyright 2016 Elsevier. (c) pH sensor, (i) transfer characteristics of the EG-CNTFET based on oxidized SWCNTs coated with the ion-selective membrane poly(1-aminoanthracene) (PAA), (ii) real-time response of the same device to different pH solutions. Reproduced with permission from Gou *et al.*, "Carbon nanotube chemiresistor for wireless pH sensing," Sci. Rep. **4**, 4468 (2014).[77] Copyright 2014 Authors, licensed under a Creative Commons Attribution (CC BY 3.0) license.

of freedom paving the way to the real-time and low-cost monitoring of different analytes, such as antigenes, biomarkers, bacteria, and ions, just to name a few. Moreover, with respect to conventional rigid electronic sensors, this novel class of FET biosensors allows integration into objects with different sizes and configurations, and, in particular, on flexible substrates using also low-cost printing methods.

While most of the EG-CNTFETs reported in this work demonstrate the high versatility of the technology, there are still several challenges to be overcome. In particular, major current issues to address are: (i) the control in the CNTs properties (size, purity, alignment); (ii) the stability of the biosensors in different environments; (iii) the detection of analytes in real-life settings, due to limitations coming from the Debye length; (iv) the optimization of the sensors design to perform multi-analyte detection in arrays.

As regards the first issue, two parameters still represent major challenges in the use of EG-CNTFETs: (1) the CNT semiconducting vs metallic purity; (2) the upper and lower limits of the CNTs diameter. The resulting high tube-to-tube variation effects in fact the device response, leading to high device-to-device variability.[26] At this regard, Salamat *et al.* have demonstrated by experimental characterization and systematic modeling that device-to-device reproducibility is highly affected by the diameter distributions of CNTs.[175] They concluded that unless the diameter distribution of the CNTs is precisely controlled, large-scale integration of CNTFET, and, in particular, of EG-CNTFET, would be difficult to achieve. In general, it is extremely important and challenging at the same time to use a high quality initial CNT material for the semiconducting layer, and at the same time to adopt optimized strategies for reliable sorting and processing of CNTs to be integrated in the FETs.[26] Novel approaches for sorting of CNTs by electronic type, diameter, and chirality are based on a combination of density gradient ultracentrifugation and solvent based separation (such as aqueous two-phase separation), where differences in hydrophobicity of surfactant-solubilized CNTs are used to achieve high fraction purity.[176,177] Additionally, the control on the alignment of CNTs as channel in FETs has also the potential to significantly impact on the sensor performances. As previously mentioned, random network of CNTs can be easily deposited, while a good control in highly dense aligned CNT arrays is still extremely challenging. In this context, innovative approaches such as biofabrication[178] are now under investigation and could find interesting application in EG-CNTFETs biosensors.

A second major challenge concerns the stability and resilience of EG-CNTFET-based biosensors over long periods and repeated stress (such as high temperature range, different pH values, potential oxidating, or reducing agents). Currently reported results are usually obtained in idealized laboratory environments with controlled environmental stimulus. When bringing these devices from the laboratory to the real-world environment with a wide-range of fluctuating parameters such as temperature, humidity, and gas compositions, these biosensors should be fully evaluated to establish their stabilities. In the context of EG-CNTFET-based biosensors, there is minimal literature on the validation of the biosensors in environments with varying buffer composition, pH, and, more importantly, physiologically relevant environments. The sensing capability of EG-FETs is usually demonstrated in PBS (pH = 7.4),[13,20,54] as this closely mimics physiological solutions.[12]

The third major challenge in EG-CNTFET-based biosensors is related to the Debye screening: as already discussed in Sec. II D, for optimal performance the sensing should happen within the λ_D.

A largely used approach is to dilute the electrolyte of the real sample to increase the λ_D. Nevertheless, in real application scenarios dilution is not the best option since the biological samples such as blood, urine, serum, and saliva contain a large amount of salts (hence a high ionic strength) and a high dilution can lead to loss of activity of biological components present in the sample.[42] More realistic approaches (especially for field applications) consist in the use of bio-recognition elements that can detect within the λ_D (e.g., fragments of antibodies or aptamers),[79,88] or in the desalting of the real sample.[93,179] However, careful optimization must be performed for the desalting process of the samples, since stable pH and ionic strength are required to ensure no degradation of the analytes.

A particularly promising approach to overcome the Debye length limitation is the co-immobilization of poly(ethylene glycol) (PEG) together with the bio-recognition element, as it enables the analyte detection at physiological ionic strength without the need for sample pretreatment (e.g., desalting).[14] The decreased effect of Debye screening from PEG is most probably attributed to the reduction of the electrolyte relative permittivity, compared to one of the water. Haustein *et al.* developed an analytical model to describe the effect of co-immobilization of PEG in reducing the Debye screening effect. The PEG effect was explained using the Donnan potential picture.[180] The combination of the bio-recognition element, linker molecules, and PEG is hypothesized to form a surface layer with a nearly constant potential. At this constant potential, the Debye screening starts further away from the sensor surface, which leads to an increased signal if the analyte binds within the PEG layer compared to the surface without PEG. This approach has successfully been used for the detection of several analytes in their physiological relevant environments.[160,181–183] Although the measured signal increase in the presence of PEG is robust and reproducible (in most of the cases threefold increase), the working principle is still not fully understood and further research is needed on this topic.[160]

Another approach that could be used to overcome the Debye length limitation, hence making possible detection at physiologically relevant concentrations, is sensing at high frequencies (e.g., 2–4 GHz).[184] Kulkarni and Zhong have presented a high-frequency CNTFET-based sensing device able to overcome the ionic screening effect by operating the sensor in the megahertz frequency range.[185] At low frequencies, the ions in the solution follow the electric field and form the EDL. However, at high frequencies, the alternating current driving force can no longer overcome the solution drag and the ions in the solution do not have sufficient time to form a stable EDL. In this case, the fluctuating dipoles of the target molecule under alternating current excitation can influence the surface potential of the CNTs, hence providing a new sensing mechanism. The authors were able to detect streptavidin binding to biotin at a buffer concentration as high as 100 mM, while operating the device at a frequency beyond 1 MHz.

In general, the demonstration of the sensing properties of EG-CNTFET-based biosensors in real-life applications is still missing in literature and really few examples of *in vivo* applications are reported. Another issue is related to the fact that the EG-FET working principle relies on what happens at all the interfaces of the device with the electrolyte, which is at the same time the dielectric and the sensing environment. Thus, as explained in Sec. II B, it is important to encapsulate the source and drain contacts from the electrolyte to avoid that the metal-CNTs contact dictates the performance of the device, instead of the CNT channel itself. Moreover, when the CNTs are exposed to the

electrolyte, a stable EDL has to be created to ensure reliable and stable measurements (stable I_{DS} vs time). However, this process usually takes time and there is no general agreement in literature about it, since very few authors clearly mention this aspect. In fact, the CNT matrix does not allow a fast permeation of the ions and CNTs not covered by the bio-recognition elements can non-selectively react with the electrolytes itself. The lack of device stability when in contact with the electrolyte needs to be surely considered and carefully evaluated.

The last major challenge regards the ability to sense multiple stimuli in a single device. This is an ultimate goal for bio- and environmental sensors and is of critical importance in the development of smart and interactive sensors that are wearable, flexible, and biocompatible. Currently, available EG-CNTFET-based biosensors have mainly focused on single or dual sensory functionalities. In fact, only a few examples of EG-CNTFET arrays and systems for the simultaneous detection of different analytes have been presented.[61] Simultaneous detection and high selectivity of multi-complex stimuli remains a challenge. This limits the applicability of these biosensors in real applications. Moreover, in the case of multiple analytes, the deduction from the obtained measurements to the desired physical/chemical quantities is not always straightforward. Selectivity of the device should be carefully evaluated against all the possible parameters, especially in complex detection environments. At this regard, the possibility to implement multiple chemistries and bio-recognition elements in EG-CNTFETs could enable new functionalities in this context.

Finally, in terms of the use of nanomaterials in biosensors, the cost needs to be lowered and their environmental effects should be carefully evaluated. Several studies have revealed that engineered nanomaterials, depending on their size, shape, surface area, chemical composition, and biopersistence, may have possible health impacts on the environment and humans. In particular, within the development of EG-CNTFET biosensors, it is important to address the concerns about the effects of CNTs on human health.[186] Various studies reported the bio-compatibility of CNTs;[187,188] however, some *in vivo* studies suggested the carcinogenicity of CNTs when inhaled.[189] This can be an issue to the handling of the materials during the devices fabrication process and its use. Thus, more studies have to be done to fully confirm the safety of this material and its application.

In addition to the still open challenges related to the fabrication and application of EG-CNTFET biosensors, progress has been made showing reproducible characteristics with biosensor sensitivities in the pM range, high selectivity, and device flexibility that could provide new opportunities for EG-CNTFET-based bioelectronics in the near future.

ACKNOWLEDGMENTS

This work was funded by the Autonomous Province of Bolzano-South Tyrol's European Regional Development Fund (ERDF) Program (project code EFRE/FESR 1127-STEX). Further funding was partially supported by the Istituto Italiano di Tecnologia (IIT) and ETH Zurich. The authors thank the Department of Innovation, Research University, and Museums of the Autonomous Province of Bozen/Bolzano for covering the Open Access publication costs.

AUTHOR DECLARATIONS

Conflict of Interest

The authors have no conflicts to disclose.

Author Contributions

B.S. and M.P. contributed equally to this work.

DATA AVAILABILITY

Data sharing is not applicable to this article as no new data were created or analyzed in this study.

REFERENCES

[1]A. Sanati, M. Jalali, K. Raeissi, F. Karimzadeh, M. Kharaziha, S. S. Mahshid, and S. Mahshid, "A review on recent advancements in electrochemical biosensing using carbonaceous nanomaterials," Microchim. Acta **186**, 773 (2019).
[2]P. Mehrotra, "Biosensors and their applications—A review," J. Oral Biol. Craniofacial Res. **6**, 153–159 (2016).
[3]A. Dudina, U. Frey, and A. Hierlemann, "Carbon-nanotube-based monolithic CMOS platform for electrochemical detection of neurotransmitter glutamate," Sensors **19**, 3080 (2019).
[4]C. S. Huertas, O. Calvo Lozano, A. Mitchell, and L. M. Lechuga, "Advanced evanescent-wave optical biosensors for the detection of nucleic acids: An analytic perspective," Front. Chem. **7**, 724 (2019).
[5]M. Pohanka, "The piezoelectric biosensors: Principles and applications," Int. J. Electrochem. Sci. **12**, 496–506 (2017).
[6]N. J. Ronkainen, H. B. Halsall, and W. R. Heineman, "Electrochemical biosensors," Chem. Soc. Rev. **39**, 1747–1763 (2010).
[7]R. Li, H. Qi, Y. Ma, Y. Deng, S. Liu, Y. Jie, J. Jing, J. He, X. Zhang, L. Wheatley *et al.*, "A flexible and physically transient electrochemical sensor for real-time wireless nitric oxide monitoring," Nat. Commun. **11**, 3207 (2020).
[8]H. Li, W. Shi, J. Song, H.-J. Jang, J. Dailey, J. Yu, and H. E. Katz, "Chemical and biomolecule sensing with organic field-effect transistors," Chem. Rev. **119**, 3–35 (2018).
[9]A. Kim, C. S. Ah, C. W. Park, J.-H. Yang, T. Kim, C.-G. Ahn, S. H. Park, and G. Y. Sung, "Direct label-free electrical immunodetection in human serum using a flow-through-apparatus approach with integrated field-effect transistors," Biosens. Bioelectron. **25**, 1767–1773 (2010).
[10]S. Cheng, S. Hideshima, S. Kuroiwa, T. Nakanishi, and T. Osaka, "Label-free detection of tumor markers using field effect transistor (FET)-based biosensors for lung cancer diagnosis," Sens. Actuators, B **212**, 329–334 (2015).
[11]C. Wang, X. Cui, Y. Li, H. Li, L. Huang, J. Bi, J. Luo, L. Q. Ma, W. Zhou, Y. Cao *et al.*, "A label-free and portable graphene FET aptasensor for children blood lead detection," Sci. Rep. **6**, 21711 (2016).
[12]M. S. Makowski and A. Ivanisevic, "Molecular analysis of blood with micro-/nanoscale field-effect-transistor biosensors," Small **7**, 1863–1875 (2011).
[13]L. Zhou, K. Wang, H. Sun, S. Zhao, X. Chen, D. Qian, H. Mao, and J. Zhao, "Novel graphene biosensor based on the functionalization of multifunctional nano-bovine serum albumin for the highly sensitive detection of cancer biomarkers," Nano-Micro Lett. **11**, 20 (2019).
[14]S. Joshi, V. D. Bhatt, H. Wu, M. Becherer, and P. Lugli, "Flexible lactate and glucose sensors using electrolyte-gated carbon nanotube field effect transistor for non-invasive real-time monitoring," IEEE Sens. J. **17**, 4315–4321 (2017).
[15]M. Salami, M. Abadi, M. Sawan, and N. Abadi, "BioFET-based integrated platform for accurate and rapid detection of e.coli bacteria: A review," J. Biosens. Bioelectron. **10**, 2 (2019).
[16]N. Nakatsuka, K.-A. Yang, J. M. Abendroth, K. M. Cheung, X. Xu, H. Yang, C. Zhao, B. Zhu, Y. S. Rim, Y. Yang *et al.*, "Aptamer–field-effect transistors overcome Debye length limitations for small-molecule sensing," Science **362**, 319–324 (2018).
[17]S. Joshi, V. D. Bhatt, A. Märtl, M. Becherer, and P. Lugli, "Regenerative, highly-sensitive, non-enzymatic dopamine sensor and impact of different buffer systems in dopamine sensing," Biosensors **8**, 9 (2018).
[18]J. Kim, M.-S. Lee, S. Jeon, M. Kim, S. Kim, K. Kim, F. Bien, S. Y. Hong, and J.-U. Park, "Highly transparent and stretchable field-effect transistor sensors using graphene–nanowire hybrid nanostructures," Adv. Mater. **27**, 3292–3297 (2015).
[19]J.-H. Jeon and W.-J. Cho, "High-performance extended-gate ion-sensitive field-effect transistors with multi-gate structure for transparent, flexible, and wearable biosensors," Sci. Technol. Adv. Mater. **21**, 371–378 (2020).

[20]C. S. Ah, C. W. Park, J.-H. Yang, J. S. Lee, W.-J. Kim, K. H. Chung, Y. H. Choi, I. B. Baek, J. Kim, and G. Y. Sung, "Detection of uncharged or feebly charged small molecules by field-effect transistor biosensors," Biosens. Bioelectron. **33**, 233–240 (2012).
[21]T. Minami, T. Sato, T. Minamiki, and S. Tokito, "An extended-gate type organic FET based biosensor for detecting biogenic amines in aqueous solution," Anal. Sci. **31**, 721–724 (2015).
[22]C. Zhao, D. Zhong, J. Han, L. Liu, Z. Zhang, and L.-M. Peng, "Exploring the performance limit of carbon nanotube network film field-effect transistors for digital integrated circuit applications," Adv. Funct. Mater. **29**, 1808574 (2019).
[23]Y. Ishige, S. Takeda, and M. Kamahori, "Direct detection of enzyme-catalyzed products by FET sensor with ferrocene-modified electrode," Biosens. Bioelectron. **26**, 1366–1372 (2010).
[24]I. Fakih, O. Durnan, F. Mahvash, I. Napal, A. Centeno, A. Zurutuza, V. Yargeau, and T. Szkopek, "Selective ion sensing with high resolution large area graphene field effect transistor arrays," Nat. Commun. **11**, 1–12 (2020).
[25]N. Liu, R. Chen, and Q. Wan, "Recent advances in electric-double-layer transistors for bio-chemical sensing applications," Sensors **19**, 3425 (2019).
[26]H. Y. Zheng, O. A. Alsager, B. Zhu, J. Travas-Sejdic, J. M. Hodgkiss, and N. O. Plank, "Electrostatic gating in carbon nanotube aptasensors," Nanoscale **8**, 13659–13668 (2016).
[27]E. Macchia, K. Manoli, B. Holzer, C. Di Franco, M. Ghittorelli, F. Torricelli, D. Alberga, G. F. Mangiatordi, G. Palazzo, G. Scamarcio *et al.*, "Single-molecule detection with a millimetre-sized transistor," Nat. Commun. **9**, 1–10 (2018).
[28]S. Sang, Y. Wang, Q. Feng, Y. Wei, J. Ji, and W. Zhang, "Progress of new label-free techniques for biosensors: A review," Crit. Rev. Biotechnol. **36**, 465–481 (2016).
[29]Q. Liu, C. Zhao, M. Chen, Y. Liu, Z. Zhao, F. Wu, Z. Li, P. S. Weiss, A. M. Andrews, and C. Zhou, "Flexible multiplexed In_2O_3 nanoribbon aptamer-field-effect transistors for biosensing," iScience **23**, 101469 (2020).
[30]A. Tibaldi, L. Fillaud, G. Anquetin, M. Woytasik, S. Zrig, B. Piro, G. Mattana, and V. Noël, "Electrolyte-gated organic field-effect transistors (EGOFETs) as complementary tools to electrochemistry for the study of surface processes," Electrochem. Commun. **98**, 43–46 (2019).
[31]J. Muñoz, F. Leonardi, T. Özmen, M. Riba-Moliner, A. González-Campo, M. Baeza, and M. Mas-Torrent, "Carbon-paste nanocomposites as unconventional gate electrodes for electrolyte-gated organic field-effect transistors: Electrical modulation and bio-sensing," J. Mater. Chem. C **7**, 14993–14998 (2019).
[32]G. Seo, G. Lee, M. J. Kim, S.-H. Baek, M. Choi, K. B. Ku, C.-S. Lee, S. Jun, D. Park, H. G. Kim *et al.*, "Rapid detection of COVID-19 causative virus (SARS-CoV-2) in human nasopharyngeal swab specimens using field-effect transistor-based biosensor," ACS Nano **14**, 5135–5142 (2020).
[33]S. Srisonphan, Y. S. Jung, and H. K. Kim, "Metal–oxide–semiconductor field-effect transistor with a vacuum channel," Nat. Nanotechnol. **7**, 504 (2012).
[34]N. Belkhamssa, C. I. Justino, P. S. Santos, S. Cardoso, I. Lopes, A. C. Duarte, T. Rocha-Santos, and M. Ksibi, "Label-free disposable immunosensor for detection of atrazine," Talanta **146**, 430–434 (2016).
[35]S. Baldo, S. Buccheri, A. Ballo, M. Camarda, A. La Magna, M. Castagna, A. Romano, D. Iannazzo, F. Di Raimondo, G. Neri *et al.*, "Carbon nanotube-based sensing devices for human arginase-1 detection," Sens. Bio-Sens. Res. **7**, 168–173 (2016).
[36]J.-H. Ahn, B. Choi, and S.-J. Choi, "Understanding the signal amplification in dual-gate FET-based biosensors," J. Appl. Phys. **128**, 184502 (2020).
[37]S.-K. Cho and W.-J. Cho, "Ultra-high sensitivity pH-sensors using silicon nanowire channel dual-gate field-effect transistors fabricated by electrospun polyvinylpyrrolidone nanofibers pattern template transfer," Sens. Actuators, B **326**, 128835 (2021).
[38]F. Scuratti, G. E. Bonacchini, C. Bossio, J. M. Salazar-Rios, W. Talsma, M. A. Loi, M. R. Antognazza, and M. Caironi, "Real-time monitoring of cellular cultures with electrolyte-gated carbon nanotube transistors," ACS Appl. Mater. Interfaces **11**, 37966–37972 (2019).
[39]T. Ozel, A. Gaur, J. A. Rogers, and M. Shim, "Polymer electrolyte gating of carbon nanotube network transistors," Nano Lett. **5**, 905–911 (2005).
[40]S. H. Kim, K. Hong, W. Xie, K. H. Lee, S. Zhang, T. P. Lodge, and C. D. Frisbie, "Electrolyte-gated transistors for organic and printed electronics," Adv. Mater. **25**, 1822–1846 (2013).
[41]L.-A. Kong, J. Sun, C. Qian, G. Gou, Y. He, J. Yang, and Y. Gao, "Ion-gel gated field-effect transistors with solution-processed oxide semiconductors for bio-inspired artificial synapses," Org. Electron. **39**, 64–70 (2016).
[42]K. Maehashi, Y. Ohno, and K. Matsumoto, "Utilizing research into electrical double layers as a basis for the development of label-free biosensors based on nanomaterial transistors," Nanobiosens. Dis. Diagn. **2016**(5), 1–13 (2015).
[43]B. G. Sonmez, O. Ertop, and S. Mutlu, "Modelling and realization of a water-gated field effect transistor (WG-FET) using 16-nm-thick mono-Si film," Sci. Rep. **7**, 1–8 (2017).
[44]L. Petti, N. Münzenrieder, C. Vogt, H. Faber, L. Büthe, G. Cantarella, F. Bottacchi, T. D. Anthopoulos, and G. Tröster, "Metal oxide semiconductor thin-film transistors for flexible electronics," Appl. Phys. Rev. **3**, 021303 (2016).
[45]Y. Yamashita, "Organic semiconductors for organic field-effect transistors," Sci. Technol. Adv. Mater. **10**, 024313 (2009).
[46]S. Chaudhury and S. K. Sinha, "Carbon nanotube and nanowires for future semiconductor devices applications," in *Nanoelectronics* (Elsevier, 2019), pp. 375–398.
[47]Q. Wang, M. Zhang, Q. Huang, Z. Liao, and C. Du, "Realizing controllable carbon nanotube arrays for soft devices by asymmetric Langmuir–Blodgett and hydrophilization process," IEEE Trans. Nanotechnol. **18**, 1144–1147 (2019).
[48]J. Zaumseil, X. Ho, J. R. Guest, G. P. Wiederrecht, and J. A. Rogers, "Electroluminescence from electrolyte-gated carbon nanotube field-effect transistors," ACS Nano **3**, 2225–2234 (2009).
[49]T. Roy, M. Tosun, J. S. Kang, A. B. Sachid, S. B. Desai, M. Hettick, C. C. Hu, and A. Javey, "Field-effect transistors built from all two-dimensional material components," ACS Nano **8**, 6259–6264 (2014).
[50]C. Klinkert, Á. Szabó, C. Stieger, D. Campi, N. Marzari, and M. Luisier, "2-D materials for ultrascaled field-effect transistors: One hundred candidates under the ab initio microscope," ACS Nano **14**, 8605–8615 (2020).
[51]Q. Cao, H.-S. Kim, N. Pimparkar, J. P. Kulkarni, C. Wang, M. Shim, K. Roy, M. A. Alam, and J. A. Rogers, "Medium-scale carbon nanotube thin-film integrated circuits on flexible plastic substrates," Nature **454**, 495–500 (2008).
[52]M. B. Lerner, J. Dailey, B. R. Goldsmith, D. Brisson, and A. C. Johnson, "Detecting lyme disease using antibody-functionalized single-walled carbon nanotube transistors," Biosens. Bioelectron. **45**, 163–167 (2013).
[53]Z. Kordrostami and M. H. Sheikhi, *Fundamental Physical Aspects of Carbon Nanotube Transistors* (InTech, 2010).
[54]V. D. Bhatt, S. Joshi, K. Melzer, and P. Lugli, "Flexible dopamine sensor based on electrolyte gated carbon nanotube field effect transistor," in *Proceedings of the 2016 IEEE Biomedical Circuits and Systems Conference (BioCAS)* (IEEE, 2016), pp. 38–41.
[55]Y. Chu, X. Wu, J. Du, and J. Huang, "Enhancement of organic field-effect transistor performance by incorporating functionalized double-walled carbon nanotubes," RSC Adv. **7**, 30626–30631 (2017).
[56]K. Maehashi, K. Matsumoto, Y. Takamura, and E. Tamiya, "Aptamer-based label-free immunosensors using carbon nanotube field-effect transistors," Electroanalysis **21**, 1285–1290 (2009).
[57]Y. Yamamoto, K. Maehashi, Y. Ohno, and K. Matsumoto, "Highly sensitive biosensors based on high-performance carbon nanotube field-effect transistors," Sens. Mater. **21**, 351–361 (2009).
[58]K. Teker, "Bioconjugated carbon nanotubes for targeting cancer biomarkers," Mater. Sci. Eng. B **153**, 83–87 (2008).
[59]K. Melzer, V. D. Bhatt, T. Schuster, E. Jaworska, K. Maksymiuk, A. Michalska, P. Lugli, and G. Scarpa, "Flexible electrolyte-gated ion-selective sensors based on carbon nanotube networks," IEEE Sens. J. **15**, 3127–3134 (2014).
[60]K. Melzer, V. Bhatt, T. Schuster, E. Jaworska, K. Maksymiuk, A. Michalska, G. Scarpa, and P. Lugli, "Multi ion-sensor arrays: Towards an 'electronic tongue,'" in *Proceedings of the 2016 IEEE 16th International Conference on Nanotechnology (IEEE-NANO)* (IEEE, 2016), pp. 475–478.
[61]K. Melzer, V. D. Bhatt, E. Jaworska, R. Mittermeier, K. Maksymiuk, A. Michalska, and P. Lugli, "Enzyme assays using sensor arrays based on ion-

selective carbon nanotube field-effect transistors," Biosens. Bioelectron. **84**, 7–14 (2016).
[62]B. L. Allen, P. D. Kichambare, and A. Star, "Carbon nanotube field-effect-transistor-based biosensors," Adv. Mater. **19**, 1439–1451 (2007).
[63]S. S. Alabsi, A. Y. Ahmed, J. O. Dennis, M. M. Khir, and A. Algamili, "A review of carbon nanotubes field effect-based biosensors," IEEE Access **8**, 69509–69521 (2020).
[64]G. Y. Wang, K. Lian, and T.-Y. Chu, "Electrolyte-gated field effect transistors in biological sensing: A survey of electrolytes," IEEE J. Electron Devices Soc. **9**, 939–950 (2021).
[65]S. Joshi, V. D. Bhatt, H. Rani, M. Becherer, and P. Lugli, "Understanding the influence of in-plane gate electrode design on electrolyte gated transistor," Microelectron. Eng. **199**, 87–91 (2018).
[66]C.-H. Chu, I. Sarangadharan, A. Regmi, Y.-W. Chen, C.-P. Hsu, W.-H. Chang, G.-Y. Lee, J.-I. Chyi, C.-C. Chen, S.-C. Shiesh *et al.*, "Beyond the Debye length in high ionic strength solution: Direct protein detection with field-effect transistors (FETs) in human serum," Sci. Rep. **7**(1), 15 (2017).
[67]K. Nagamine, A. Nomura, Y. Ichimura, R. Izawa, S. Sasaki, H. Furusawa, H. Matsui, and S. Tokito, "Printed organic transistor-based biosensors for non-invasive sweat analysis," Anal. Sci. **36**, 291–302 (2020).
[68]S. Sheibani, L. Capua, S. Kamaei, S. S. A. Akbari, J. Zhang, H. Guerin, and A. M. Ionescu, "Extended gate field-effect-transistor for sensing cortisol stress hormone," Commun. Mater. **2**, 1–10 (2021).
[69]N. T. Tung, P. T. Tue, T. T. N. Lien, Y. Ohno, K. Maehashi, K. Matsumoto, K. Nishigaki, M. Biyani, and Y. Takamura, "Peptide aptamer-modified single-walled carbon nanotube-based transistors for high-performance biosensors," Sci. Rep. **7**, 1–9 (2017).
[70]M. Pacios, I. Martin-Fernandez, X. Borrisé, M. del Valle, J. Bartrolí, E. Lora-Tamayo, P. Godignon, F. Pérez-Murano, and M. J. Esplandiu, "Real time protein recognition in a liquid-gated carbon nanotube field-effect transistor modified with aptamers," Nanoscale **4**, 5917–5923 (2012).
[71]S. Rosenblatt, Y. Yaish, J. Park, J. Gore, V. Sazonova, and P. L. McEuen, "High performance electrolyte gated carbon nanotube transistors," Nano Lett. **2**, 869–872 (2002).
[72]I. Heller, A. M. Janssens, J. Männik, E. D. Minot, S. G. Lemay, and C. Dekker, "Identifying the mechanism of biosensing with carbon nanotube transistors," Nano Lett. **8**, 591–595 (2008).
[73]A. Palaniappan, W. Goh, J. Tey, I. Wijaya, S. Moochhala, B. Liedberg, and S. Mhaisalkar, "Aligned carbon nanotubes on quartz substrate for liquid gated biosensing," Biosens. Bioelectron. **25**, 1989–1993 (2010).
[74]A. Palaniappan, W. Goh, D. Fam, G. Rajaseger, C. Chan, B. Hanson, S. Moochhala, S. Mhaisalkar, and B. Liedberg, "Label-free electronic detection of bio-toxins using aligned carbon nanotubes," Biosens. Bioelectron. **43**, 143–147 (2013).
[75]K. Maehashi, T. Katsura, K. Kerman, Y. Takamura, K. Matsumoto, and E. Tamiya, "Label-free protein biosensor based on aptamer-modified carbon nanotube field-effect transistors," Anal. Chem. **79**, 782–787 (2007).
[76]D. Cao, P. Pang, H. Liu, J. He, and S. Lindsay, "Electronic sensitivity of a single-walled carbon nanotube to internal electrolyte composition," Nanotechnology **23**, 085203 (2012).
[77]P. Gou, N. D. Kraut, I. M. Feigel, H. Bai, G. J. Morgan, Y. Chen, Y. Tang, K. Bocan, J. Stachel, L. Berger *et al.*, "Carbon nanotube chemiresistor for wireless pH sensing," Sci. Rep. **4**, 4468 (2014).
[78]J.-H. Jin, J. Kim, T. Jeon, S.-K. Shin, J.-R. Sohn, H. Yi, and B. Y. Lee, "Real-time selective monitoring of allergenic aspergillus molds using pentameric antibody-immobilized single-walled carbon nanotube-field effect transistors," RSC Adv. **5**, 15728–15735 (2015).
[79]J. P. Kim, B. Y. Lee, S. Hong, and S. J. Sim, "Ultrasensitive carbon nanotube-based biosensors using antibody-binding fragments," Anal. Biochem. **381**, 193–198 (2008).
[80]G. Lee, J. Lim, J. Park, S. Choi, S. Hong, and H. Park, "Neurotransmitter detection by enzyme-immobilized CNT-FET," Curr. Appl. Phys. **9**, S25–S28 (2009).
[81]Y. Cho, V. A. Pham Ba, J.-Y. Jeong, Y. Choi, and S. Hong, "Ion-selective carbon nanotube field-effect transistors for monitoring drug effects on nicotinic acetylcholine receptor activation in live cells," Sensors **20**, 3680 (2020).
[82]D. Lee and T. Cui, "Low-cost, transparent, and flexible single-walled carbon nanotube nanocomposite based ion-sensitive field-effect transistors for pH/glucose sensing," Biosens. Bioelectron. **25**, 2259–2264 (2010).
[83]K. Melzer, A. Münzer, E. Jaworska, K. Maksymiuk, A. Michalska, and G. Scarpa, "Selective ion-sensing with membrane-functionalized electrolyte-gated carbon nanotube field-effect transistors," Analyst **139**, 4947–4954 (2014).
[84]V. D. Bhatt, S. Joshi, and P. Lugli, "Metal-free fully solution-processable flexible electrolyte-gated carbon nanotube field effect transistor," IEEE Trans. Electron Devices **64**, 1375–1379 (2017).
[85]V. D. Bhatt, S. Joshi, M. Becherer, and P. Lugli, "Flexible, low-cost sensor based on electrolyte gated carbon nanotube field effect transistor for organophosphate detection," Sensors **17**, 1147 (2017).
[86]E. Stelmach, E. Jaworska, V. D. Bhatt, M. Becherer, P. Lugli, A. Michalska, and K. Maksymiuk, "Electrolyte gated transistors modified by polypyrrole nanoparticles," Electrochim. Acta **309**, 65–73 (2019).
[87]C.-S. Lee, Y. Ju, J. Kim, and T. H. Kim, "Electrochemical functionalization of single-walled carbon nanotubes with amine-terminated dendrimers encapsulating pt nanoparticles: Toward facile field-effect transistor-based sensing platforms," Sens. Actuators, B **275**, 367–372 (2018).
[88]F. Khosravi, S. M. Loeian, and B. Panchapakesan, "Ultrasensitive label-free sensing of IL-6 based on PASE functionalized carbon nanotube micro-arrays with RNA-aptamers as molecular recognition elements," Biosensors **7**, 17 (2017).
[89]S. Makarychev-Mikhailov, A. Shvarev, and E. Bakker, "CHAPTER 4—New trends in ion-selective electrodes," in *Electrochemical Sensors, Biosensors and their Biomedical Applications*, edited by X. Zhang, H. Ju, and J. Wang (Academic Press, San Diego, 2008), pp. 71–114.
[90]L. Suo, O. Borodin, T. Gao, M. Olguin, J. Ho, X. Fan, C. Luo, C. Wang, and K. Xu, "'Water-in-salt' electrolyte enables high-voltage aqueous lithium-ion chemistries," Science **350**, 938–943 (2015).
[91]L. Hu, D. S. Hecht, and G. Gruner, "Carbon nanotube thin films: Fabrication, properties, and applications," Chem. Rev. **110**, 5790–5844 (2010).
[92]K. B. Oldham, "A Gouy–Chapman–Stern model of the double layer at a (metal)/(ionic liquid) interface," J. Electroanal. Chem. **613**, 131–138 (2008).
[93]A. C. M. De Moraes and L. T. Kubota, "Recent trends in field-effect transistors-based immunosensors," Chemosensors **4**, 20 (2016).
[94]F. Loghin, S. Colasanti, A. Weise, A. Falco, A. Abdelhalim, P. Lugli, and A. Abdellah, "Scalable spray deposition process for highly uniform and reproducible CNT-TFTs," Flexible Printed Electron. **1**, 045002 (2016).
[95]G. Cantarella, N. Münzenrieder, L. Petti, C. Vogt, L. Büthe, G. Salvatore, A. Daus, and G. Tröster, "Flexible In–Ga–Zn–O thin-film transistors on elastomeric substrate bent to 2.3% strain," IEEE Electron Device Lett. **36**, 781–783 (2015).
[96]R. Koul, M. Yadav, and R. Pandey, "Comparative analysis of MOSFET, FINFET and GAAFET devices using different substrate and gate oxide materials," in *Innovations in Electrical and Electronic Engineering*, edited by S. Mekhilef, M. Favorskaya, R. K. Pandey, and R. N. Shaw (Springer, Singapore, 2021), pp. 417–430.
[97]V. Schroeder, S. Savagatrup, M. He, S. Lin, and T. M. Swager, "Carbon nanotube chemical sensors," Chem. Rev. **119**, 599–663 (2018).
[98]A. Shrivastava and V. Gupta, "Methods for the determination of limit of detection and limit of quantitation of the analytical methods," Chronicles Young Sci. **2**, 21–21 (2011).
[99]N. Saifuddin, A. Raziah, and A. Junizah, "Carbon nanotubes: A review on structure and their interaction with proteins," J. Chem. **2013**, 676815.
[100]N. Anzar, R. Hasan, M. Tyagi, N. Yadav, and J. Narang, "Carbon nanotube—A review on synthesis, properties and plethora of applications in the field of biomedical science," Sens. Int. **1**, 100003 (2020).
[101]I. V. Zaporotskova, N. P. Boroznina, Y. N. Parkhomenko, and L. V. Kozhitov, "Carbon nanotubes: Sensor properties. A review," Mod. Electron. Mater. **2**, 95–105 (2016).
[102]P. G. Collins and P. Avouris, "The electronic properties of carbon nanotubes," Contemp. Concepts Condens. Matter Sci. **3**, 49–81 (2008).
[103]M. Dresselhaus, R. Saito, and A. Jorio, "Semiconducting carbon nanotubes," AIP Conf. Proc. **772**, 25–31 (2005).

[104]L.-M. Peng, Z. Zhang, and C. Qiu, "Carbon nanotube digital electronics," Nat. Electron. **2**, 499–505 (2019).
[105]M. Ahmad and S. R. P. Silva, "Low temperature growth of carbon nanotubes—A review," Carbon **158**, 24–44 (2020).
[106]S. Zhang, L. Kang, X. Wang, L. Tong, L. Yang, Z. Wang, K. Qi, S. Deng, Q. Li, X. Bai *et al.*, "Arrays of horizontal carbon nanotubes of controlled chirality grown using designed catalysts," Nature **543**, 234–238 (2017).
[107]X. Zhao, X. Liu, F. Yang, Q. Liu, Z. Zhang, and Y. Li, "Graphene oxide-supported cobalt tungstate as catalyst precursor for selective growth of single-walled carbon nanotubes," Inorg. Chem. Front. **8**, 940–946 (2021).
[108]E. Dervishi, Z. Li, Y. Xu, V. Saini, A. R. Biris, D. Lupu, and A. S. Biris, "Carbon nanotubes: Synthesis, properties, and applications," Part. Sci. Technol. **27**, 107–125 (2009).
[109]K. Awasthi, A. Srivastava, and O. Srivastava, "Synthesis of carbon nanotubes," J. Nanosci. Nanotechnol. **5**, 1616–1636 (2005).
[110]J. Ouyang, J. Ding, J. Lefebvre, Z. Li, C. Guo, A. J. Kell, and P. R. Malenfant, "Sorting of semiconducting single-walled carbon nanotubes in polar solvents with an amphiphilic conjugated polymer provides general guidelines for enrichment," ACS Nano **12**, 1910–1919 (2018).
[111]D. Liu, P. Li, X. Yu, J. Gu, J. Han, S. Zhang, H. Li, H. Jin, S. Qiu, Q. Li *et al.*, "A mixed-extractor strategy for efficient sorting of semiconducting single-walled carbon nanotubes," Adv. Mater. **29**, 1603565 (2017).
[112]L. Liu, J. Han, L. Xu, J. Zhou, C. Zhao, S. Ding, H. Shi, M. Xiao, L. Ding, Z. Ma *et al.*, "Aligned, high-density semiconducting carbon nanotube arrays for high-performance electronics," Science **368**, 850–856 (2020).
[113]H. Wang and Z. Bao, "Conjugated polymer sorting of semiconducting carbon nanotubes and their electronic applications," Nano Today **10**, 737–758 (2015).
[114]S. Mesgari, A. K. Sundramoorthy, L. S. Loo, and M. B. Chan-Park, "Gel electrophoresis using a selective radical for the separation of single-walled carbon nanotubes," Faraday Discuss. **173**, 351–363 (2014).
[115]S. Ghosh, S. M. Bachilo, and R. B. Weisman, "Advanced sorting of single-walled carbon nanotubes by nonlinear density-gradient ultracentrifugation," Nat. Nanotechnol. **5**, 443–450 (2010).
[116]Q. Cao and J. A. Rogers, "Random networks and aligned arrays of single-walled carbon nanotubes for electronic device applications," Nano Res. **1**, 259–272 (2008).
[117]H.-K. Jang, J. E. Jin, J. H. Choi, P.-S. Kang, D.-H. Kim, and G. T. Kim, "Electrical percolation thresholds of semiconducting single-walled carbon nanotube networks in field-effect transistors," Phys. Chem. Chem. Phys. **17**, 6874–6880 (2015).
[118]M. A. Topinka, M. W. Rowell, D. Goldhaber-Gordon, M. D. McGehee, D. S. Hecht, and G. Gruner, "Charge transport in interpenetrating networks of semiconducting and metallic carbon nanotubes," Nano Lett. **9**, 1866–1871 (2009).
[119]S.-J. Choi, C. Wang, C. C. Lo, P. Bennett, A. Javey, and J. Bokor, "Comparative study of solution-processed carbon nanotube network transistors," Appl. Phys. Lett. **101**, 112104 (2012).
[120]M. A. Barik, R. Deka, and J. C. Dutta, "Carbon nanotube-based dual-gated junctionless field-effect transistor for acetylcholine detection," IEEE Sens. J. **16**, 280–286 (2015).
[121]X. Zhang, D. Wang, D. Yang, S. Li, Z. Shen *et al.*, "Electronic detection of Escherichia coli o157:h7 using single-walled carbon nanotubes field-effect transistor biosensor," Engineering **4**, 94 (2013).
[122]M. Zhao, Y. Chen, K. Wang, Z. Zhang, J. K. Streit, J. A. Fagan, J. Tang, M. Zheng, C. Yang, Z. Zhu *et al.*, "DNA-directed nanofabrication of high-performance carbon nanotube field-effect transistors," Science **368**, 878–881 (2020).
[123]C. Kocabas, S.-H. Hur, A. Gaur, M. A. Meitl, M. Shim, and J. A. Rogers, "Guided growth of large-scale, horizontally aligned arrays of single-walled carbon nanotubes and their use in thin-film transistors," Small **1**, 1110–1116 (2005).
[124]A. Rivadeneyra, F. C. Loghin, and A. Falco, "Technological integration in printed electronics," in *Flexible Electronics* (IntechOpen, 2018).
[125]A. Abdellah, A. Abdelhalim, F. Loghin, P. Köhler, Z. Ahmad, G. Scarpa, and P. Lugli, "Flexible carbon nanotube based gas sensors fabricated by large-scale spray deposition," IEEE Sens. J. **13**, 4014–4021 (2013).
[126]A. Abdelhalim, M. Winkler, F. Loghin, C. Zeiser, P. Lugli, and A. Abdellah, "Highly sensitive and selective carbon nanotube-based gas sensor arrays functionalized with different metallic nanoparticles," Sens. Actuators, B **220**, 1288–1296 (2015).
[127]Q. Cao and J. A. Rogers, "Ultrathin films of single-walled carbon nanotubes for electronics and sensors: A review of fundamental and applied aspects," Adv. Mater. **21**, 29–53 (2009).
[128]Y. B. Pottathara, Y. Grohens, V. Kokol, N. Kalarikkal, and S. Thomas, "Synthesis and processing of emerging two-dimensional nanomaterials," in *Nanomaterials Synthesis* (Elsevier, 2019), pp. 1–25.
[129]Z. Cai, B. Liu, X. Zou, and H.-M. Cheng, "Chemical vapor deposition growth and applications of two-dimensional materials and their heterostructures," Chem. Rev. **118**, 6091–6133 (2018).
[130]M. Kumar and Y. Ando, "Chemical vapor deposition of carbon nanotubes: A review on growth mechanism and mass production," J. Nanosci. Nanotechnol. **10**, 3739–3758 (2010).
[131]T. Zhou, E. Kropp, J. Chen, and L. Kulinsky, "Step-wise deposition process for dielectrophoretic formation of conductive 50-μm-long carbon nanotube bridges," Micromachines **11**, 371 (2020).
[132]W. Xue and P. Li, "Dielectrophoretic deposition and alignment of carbon nanotubes," in *Carbon Nanotubes-Synthesis, Characterization, Applications* (IntechOpen, 2011), pp. 171–190.
[133]J. Kimbrough, S. Chance, B. Whitaker, Z. Duncan, K. Davis, A. Henderson, Z. Xiao, Q. Yuan, and F. Camino, "Deposition and alignment of carbon nanotubes with dielectrophoresis for fabrication of carbon nanotube field-effect transistors," in *Proceedings of the 2018 IEEE International Conference on Manipulation, Manufacturing and Measurement on the Nanoscale (3M-NANO)* (IEEE, 2018), pp. 308–311.
[134]F. Tournus, S. Latil, M. Heggie, and J.-C. Charlier, "π-stacking interaction between carbon nanotubes and organic molecules," Phys. Rev. B **72**, 075431 (2005).
[135]K. Matsuura, T. Saito, T. Okazaki, S. Ohshima, M. Yumura, and S. Iijima, "Selectivity of water-soluble proteins in single-walled carbon nanotube dispersions," Chem. Phys. Lett. **429**, 497–502 (2006).
[136]S. Stefansson, H. H. Kwon, and S. N. Ahn, "Targeting antibodies to carbon nanotube field effect transistors by pyrene hydrazide modification of heavy chain carbohydrates," J. Nanotechnol. **2012**, 490175.
[137]B. Huang, "Carbon nanotubes and their polymeric composites: The applications in tissue engineering," Biomanuf. Rev. **5**, 1–26 (2020).
[138]R. Konradi, M. Textor, and E. Reimhult, "Using complementary acoustic and optical techniques for quantitative monitoring of biomolecular adsorption at interfaces," Biosensors **2**, 341–376 (2012).
[139]C. I. Cheng, Y.-P. Chang, and Y.-H. Chu, "Biomolecular interactions and tools for their recognition: Focus on the quartz crystal microbalance and its diverse surface chemistries and applications," Chem. Soc. Rev. **41**, 1947–1971 (2012).
[140]D. K. H. Tsang, T. J. Lieberthal, C. Watts, I. E. Dunlop, S. Ramadan, E. Armando, and N. Klein, "Chemically functionalised graphene FET biosensor for the label-free sensing of exosomes," Sci. Rep. **9**, 1–10 (2019).
[141]R. Haddad, S. Cosnier, A. Maaref, and M. Holzinger, "Non-covalent biofunctionalization of single-walled carbon nanotubes via biotin attachment by π-stacking interactions and pyrrole polymerization," Analyst **134**, 2412–2418 (2009).
[142]J. Vörös, J. Ramsden, G. Csúcs, I. Szendrő, S. De Paul, M. Textor, and N. Spencer, "Optical grating coupler biosensors," Biomaterials **23**, 3699–3710 (2002).
[143]M. A. Morales and J. M. Halpern, "Guide to selecting a biorecognition element for biosensors," Bioconjugate Chem. **29**, 3231–3239 (2018).
[144]J. Herlet, P. Kornberger, B. Roessler, J. Glanz, W. Schwarz, W. Liebl, and V. Zverlov, "A new method to evaluate temperature vs. pH activity profiles for biotechnological relevant enzymes," Biotechnol. Biofuels **10**, 1–12 (2017).
[145]X. Luo and J. J. Davis, "Electrical biosensors and the label free detection of protein disease biomarkers," Chem. Soc. Rev. **42**, 5944–5962 (2013).
[146]M. Butler, "Hybridomas, genetic engineering of," in *Encyclopedia of Physical Science and Technology*, edited by R. A. Meyers, 3rd ed. (Academic Press, New York, 2003), pp. 427–443.
[147]C. Tuerk and L. Gold, "Systematic evolution of ligands by exponential enrichment: RNA ligands to bacteriophage T4 DNA polymerase," Science **249**, 505–510 (1990).

[148]A. D. Ellington and J. W. Szostak, "In vitro selection of rna molecules that bind specific ligands," Nature **346**, 818–822 (1990).
[149]T. Mairal Lerga, M. Jauset-Rubio, V. Skouridou, A. S. Bashammakh, M. S. El-Shahawi, A. O. Alyoubi, and C. K. O'Sullivan, "High affinity aptamer for the detection of the biogenic amine histamine," Anal. Chem. **91**, 7104–7111 (2019).
[150]M. Fatin, A. R. Ruslinda, S. C. Gopinath, and M. M. Arshad, "High-performance interactive analysis of split aptamer and HIV-1 Tat on multiwall carbon nanotube-modified field-effect transistor," Int. J. Biol. Macromol. **125**, 414–422 (2019).
[151]F. Odeh, H. Nsairat, W. Alshaer, M. A. Ismail, E. Esawi, B. Qaqish, A. A. Bawab, and S. I. Ismail, "Aptamers chemistry: Chemical modifications and conjugation strategies," Molecules **25**, 3 (2020).
[152]N. Arroyo-Currás, J. Somerson, P. A. Vieira, K. L. Ploense, T. E. Kippin, and K. W. Plaxco, "Real-time measurement of small molecules directly in awake, ambulatory animals," Proc. Natl. Acad. Sci. **114**, 645–650 (2017).
[153]N. Nakatsuka, A. Faillétaz, D. Eggemann, C. Forró, J. Vörös, and D. Momotenko, "Aptamer conformational change enables serotonin biosensing with nanopipettes," Anal. Chem. **93**, 4033–4041 (2021).
[154]N. Nakatsuka, K. J. Heard, A. Faillétaz, D. Momotenko, J. Vörös, F. H. Gage, and K. C. Vadodaria, "Sensing serotonin secreted from human serotonergic neurons using aptamer-modified nanopipettes," Mol. Psychiatry **26**, 2753–2763 (2021).
[155]N. Qiao, J. Li, X. Wu, D. Diao, J. Zhao, J. Li, X. Ren, X. Ding, D. Shangguan, and X. Lou, "Speeding up in vitro discovery of structure-switching aptamers via magnetic cross-linking precipitation," Anal. Chem. **91**, 13383–13389 (2019).
[156]E. S. Coonahan, K.-A. Yang, S. Pecic, M. De Vos, T. E. Wellems, M. P. Fay, J. F. Andersen, J. Tarning, and C. A. Long, "Structure-switching aptamer sensors for the specific detection of piperaquine and mefloquine," Sci. Transl. Med. **13**, 1–12 (2021).
[157]K.-A. Yang, R. Pei, D. Stefanovic, and M. N. Stojanovic, "Optimizing cross-reactivity with evolutionary search for sensors," J. Am. Chem. Soc. **134**, 1642–1647 (2012).
[158]D. T. Jackson and P. N. Nelson, "Preparation and properties of some ion selective membranes: A review," J. Mol. Struct. **1182**, 241–259 (2019).
[159]K. Mikhelson, "Ion-selective electrodes in PVC matrix," Sens. Actuators, B **18**, 31–37 (1994).
[160]M. S. Filipiak, M. Rother, N. M. Andoy, A. C. Knudsen, S. Grimm, C. Bachran, L. K. Swee, J. Zaumseil, and A. Tarasov, "Highly sensitive, selective and label-free protein detection in physiological solutions using carbon nanotube transistors with nanobody receptors," Sens. Actuators, B **255**, 1507–1516 (2018).
[161]E. Fernandes, P. D. Cabral, R. Campos, G. Machado, Jr., M. F. Cerqueira, C. Sousa, P. P. Freitas, J. Borme, D. Y. Petrovykh, and P. Alpuim, "Functionalization of single-layer graphene for immunoassays," Appl. Surf. Sci. **480**, 709–716 (2019).
[162]A. Frutiger, A. Tanno, S. Hwu, R. F. Tiefenauer, J. Vörös, and N. Nakatsuka, "Nonspecific binding-fundamental concepts and consequences for biosensing applications," Chem. Rev. **121**, 8095–8160 (2021).
[163]S. Joshi, V. D. Bhatt, E. Jaworska, M. Becherer, K. Maksymiuk, A. Michalska, and P. Lugli, "Using lipophilic membrane for enhanced-performance aqueous gated carbon nanotube field effect transistors," Phys. Status Solidi A **215**, 1700993 (2018).
[164]J. M. Fowler, D. K. Wong, H. B. Halsall, and W. R. Heineman, "Recent developments in electrochemical immunoassays and immunosensors," in *Electrochemical Sensors, Biosensors and their Biomedical Applications* (Academic Press, 2008), pp. 115–143.
[165]S. Shigdar, J. Macdonald, M. O'Connor, T. Wang, D. Xiang, L. Qiao, M. Wei, S.-F. Zhou, Y. Zhu, L. Kong *et al.*, "Aptamers as theranostic agents: Modifications, serum stability and functionalisation," Sensors **13**, 13624–13637 (2013).
[166]S. F. Peteu, S. Szunerits, A. Vasilescu, and W. Knoll, "Nanoscale architectures for smart bio-interfaces: Advances and challenges," in *Nanofabrication Intech*, edited by Y. Masuda (IntechOpen, 2011), pp. 63–98.
[167]J. Lee, M. Jo, T. H. Kim, J.-Y. Ahn, D.-K. Lee, S. Kim, and S. Hong, "Aptamer sandwich-based carbon nanotube sensors for single-carbon-atomic-resolution detection of non-polar small molecular species," Lab Chip **11**, 52–56 (2011).
[168]B. K. Das, C. Tlili, S. Badhulika, L. N. Cella, W. Chen, and A. Mulchandani, "Single-walled carbon nanotubes chemiresistor aptasensors for small molecules: Picomolar level detection of adenosine triphosphate," Chem. Commun. **47**, 3793–3795 (2011).
[169]S. G. Kim, J. S. Lee, J. Jun, D. H. Shin, and J. Jang, "Ultrasensitive bisphenol a field-effect transistor sensor using an aptamer-modified multichannel carbon nanofiber transducer," ACS Appl. Mater. Interfaces **8**, 6602–6610 (2016).
[170]A. R. Thompson, D. L. Enfield, L. H. Ericsson, M. E. Legaz, and J. W. Fenton II, "Human thrombin: Partial primary structure," Arch. Biochem. Biophys. **178**, 356–367 (1977).
[171]A. Geiger, P. Burgstaller, H. Von der Eltz, A. Roeder, and M. Famulok, "RNA aptamers that bind l-arginine with sub-micromolar dissociation constants and high enantioselectivity," Nucl. Acids Res. **24**, 1029–1036 (1996).
[172]R. J. White and K. W. Plaxco, "Engineering new aptamer geometries for electrochemical aptamer-based sensors," in *Bio-Inspired/Biomimetic Sensor Technologies and Applications* (International Society for Optics and Photonics, 2009), Vol. 7321, p. 732105.
[173]C. C. Cid, J. Riu, A. Maroto, and F. X. Rius, "Ion-sensitive field effect transistors using carbon nanotubes as the transducing layer," Analyst **133**, 1001–1004 (2008).
[174]H. S. White, G. P. Kittlesen, and M. S. Wrighton, "Chemical derivatization of an array of three gold microelectrodes with polypyrrole: Fabrication of a molecule-based transistor," J. Am. Chem. Soc. **106**, 5375–5377 (1984).
[175]S. Salamat, X. Ho, J. A. Rogers, and M. A. Alam, "Intrinsic performance variability in aligned array CNFETs," IEEE Trans. Nanotechnol. **10**, 439–444 (2010).
[176]H. Li, G. Gordeev, O. Garrity, N. A. Peyyety, P. B. Selvasundaram, S. Dehm, R. Krupke, S. Cambré, W. Wenseleers, S. Reich *et al.*, "Separation of specific single-enantiomer single-wall carbon nanotubes in the large-diameter regime," ACS Nano **14**, 948–963 (2020).
[177]J. A. Fagan, "Aqueous two-polymer phase extraction of single-wall carbon nanotubes using surfactants," Nanoscale Adv. **1**, 3307–3324 (2019).
[178]X. Dai, Q. Li, A. Aldalbahi, L. Wang, C. Fan, and X. Liu, "DNA-based fabrication for nanoelectronics," Nano Lett. **20**, 5604–5615 (2020).
[179]Y.-W. Huang, C.-S. Wu, C.-K. Chuang, S.-T. Pang, T.-M. Pan, Y.-S. Yang, and F.-H. Ko, "Real-time and label-free detection of the prostate-specific antigen in human serum by a polycrystalline silicon nanowire field-effect transistor biosensor," Anal. Chem. **85**, 7912–7918 (2013).
[180]N. Haustein, Ó. Gutiérrez-Sanz, and A. Tarasov, "Analytical model to describe the effect of polyethylene glycol on ionic screening of analyte charges in transistor-based immunosensing," ACS Sensors **4**, 874–882 (2019).
[181]N. M. Andoy, M. S. Filipiak, D. Vetter, Ó. Gutiérrez-Sanz, and A. Tarasov, "Graphene-based electronic immunosensor with femtomolar detection limit in whole serum," Adv. Mater. Technol. **3**, 1800186 (2018).
[182]N. Gao, T. Gao, X. Yang, X. Dai, W. Zhou, A. Zhang, and C. M. Lieber, "Specific detection of biomolecules in physiological solutions using graphene transistor biosensors," Proc. Natl. Acad. Sci. **113**, 14633–14638 (2016).
[183]M.-Á. García-Chamé, Ó. Gutiérrez-Sanz, E. Ercan-Herbst, N. Haustein, M. S. Filipiak, D. E. Ehrnhöfer, and A. Tarasov, "A transistor-based label-free immunosensor for rapid detection of tau protein," Biosens. Bioelectron. **159**, 112129 (2020).
[184]W. Fu, M. El Abbassi, T. Hasler, M. Jung, M. Steinacher, M. Calame, C. Schönenberger, G. Puebla-Hellmann, S. Hellmüller, T. Ihn *et al.*, "Electrolyte gate dependent high-frequency measurement of graphene field-effect transistor for sensing applications," Appl. Phys. Lett. **104**, 013102 (2014).
[185]G. S. Kulkarni and Z. Zhong, "Detection beyond the Debye screening length in a high-frequency nanoelectronic biosensor," Nano Lett. **12**, 719–723 (2012).
[186]K. Aoki and N. Saito, "Biocompatibility and carcinogenicity of carbon nanotubes as biomaterials," Nanomaterials **10**, 264 (2020).
[187]A. Murray, E. Kisin, S. Leonard, S. Young, C. Kommineni, V. Kagan, V. Castranova, and A. Shvedova, "Oxidative stress and inflammatory response in

dermal toxicity of single-walled carbon nanotubes," Toxicology **257**, 161–171 (2009).
[188]S. Nahle, R. Safar, S. Grandemange, B. Foliguet, M. Lovera-Leroux, Z. Doumandji, A. Le Faou, O. Joubert, B. Rihn, and L. Ferrari, "Single wall and multiwall carbon nanotubes induce different toxicological responses in rat alveolar macrophages," J. Appl. Toxicol. **39**, 764–772 (2019).
[189]M. Barbarino and A. Giordano, "Assessment of the carcinogenicity of carbon nanotubes in the respiratory system," Cancers **13**, 1318 (2021).